

General Disclaimer

One or more of the Following Statements may affect this Document

- This document has been reproduced from the best copy furnished by the organizational source. It is being released in the interest of making available as much information as possible.
- This document may contain data, which exceeds the sheet parameters. It was furnished in this condition by the organizational source and is the best copy available.
- This document may contain tone-on-tone or color graphs, charts and/or pictures, which have been reproduced in black and white.
- This document is paginated as submitted by the original source.
- Portions of this document are not fully legible due to the historical nature of some of the material. However, it is the best reproduction available from the original submission.

USE OF THERMAL INERTIA DETERMINED BY HCMM TO PREDICT NOCTURNAL COLD PRONE AREAS IN FLORIDA

E84-10005
CR-174520

HCMM DATA INVESTIGATION HFO-002
CONTRACT NAS5-26453

"Made available under NASA sponsorship
in the interest of early and wide dis-
semination of Earth Resources Survey
Program information and without liability
for any use made thereof."

L.H. Allen, Jr., Principal Investigator
University of Florida
Institute of Food and Agricultural Sciences
Building 164, Agronomy Physiology Lab.
Gainesville, FL 32611

(E84-10005) USE OF THERMAL INERTIA
DETERMINED BY HCMM TO PREDICT NOCTURNAL COLD
PRONE AREAS IN FLORIDA Final Report, Mar.
1981 - Mar. 1983 (Florida Univ.) 74 p
HC A03/MF A01

N84-11546

Unclass
00005

CSSL 05B G3/43

Coinvestigators

Ellen Chen, Cooperator, Research Associate
J.D. Martsolf, Cooperator, Professor, Fruit Crops Department
P.H. Jones, Cooperator, Research Associate
Toby N. Carlson, Cooperator, Professor, Meteorology Department,
Pennsylvania State University

October 1983
Final Report, March 1981 to March 1983



Prepared for
NATIONAL AERONAUTICS AND SPACE ADMINISTRATION
GODDARD SPACE FLIGHT CENTER
Greenbelt, MD 20771

USE OF THERMAL INERTIA DETERMINED BY HCMM TO PREDICT NOCTURNAL COLD
PRONE AREAS IN FLORIDA

HCMM DATA INVESTIGATION HFO-002
CONTRACT NAS5-26453

L.H. Allen, Jr., Principal Investigator
University of Florida
Institute of Food and Agricultural Sciences
Building 164, Agronomy Physiology Lab.
Gainesville, FL 32611

Coinvestigators

Ellen Chen, Cooperator, Research Associate
J.D. Martsolf, Cooperator, Professor, Fruit Crops Department
P.H. Jones, Cooperator, Research Associate
Toby N. Carlson, Cooperator, Professor, Meteorology Department,
Pennsylvania State University

Original photography may be purchased
from EOS Data Center
Sioux Falls, SD 57199

October 1983
Final Report, March 1981 to March 1983

Prepared for
NATIONAL AERONAUTICS AND SPACE ADMINISTRATION
GODDARD SPACE FLIGHT CENTER
Greenbelt, MD 20771

TECHNICAL REPORT STANDARD TITLE PAGE

1. Report No.	2. Government Accession No.	3. Recipient's Catalog No.	
4. Title and Subtitle USE OF THERMAL INERTIA DETERMINED BY HCMM TO PREDICT NOCTURNAL COLD-PRONE AREAS IN FLORIDA		5. Report Date October 1983	6. Performing Organization Code
7. Author(s) L.H. Allen, Jr., et al.		8. Performing Organization Report No.	
9. Performing Organization Name and Address Institute of Food and Agricultural Sciences University of Florida Gainesville, FL 32611		10. Work Unit No.	
		11. Contract or Grant No. NAS5-26453	
		13. Type of Report and Period Covered TYPE III Final Report March 1981 to March 1983	
12. Sponsoring Agency Name and Address National Aeronautics and Space Administration Goddard Space Flight Center Greenbelt, MD 20771		14. Sponsoring Agency Code	
15. Supplementary Notes Prepared in cooperation with the Soil and Water Research Unit, Agricultural Research Service, U.S. Department of Agriculture, at Gainesville Florida, through AGRISTARS (Early Warning/Crop Condition Assessment).			
16. Abstract The Heat Capacity Mapping Mission (HCMM) satellite was launched on April 26, 1978, in a polar orbit with nominal equatorial ascending and descending crossing times of 2:00 pm and 2:00 am, respectively. Pairs of HCMM day-night thermal infrared (IR) data were selected during the 1978-79 winter to examine patterns of surface temperature and thermal inertia (TI) of peninsular Florida. GOES and NOAA-6 thermal IR, as well as National Climatic Center temperatures and rainfall, were also used. HCMM apparent thermal inertia (ATI) images closely corresponded to the General Soil Map of Florida, based on soil drainage classes. Areas with low ATI overlay well-drained soils, such as deep sands and drained organic soils, whereas areas with high ATI overlay areas with wetlands and bodies of water. The HCMM ATI images also corresponded well with GOES-detected winter nocturnal cold-prone areas. Use of HCMM data with Carlson's energy balance model showed both high moisture availability (MA) and high thermal inertia (TI) of wetland-type surfaces and low MA and low TI of upland, well-drained soils. Since soil areas with low TI develop higher temperatures during the day, then antecedent patterns of highest maximum daytime surface temperature can also be used to predict nocturnal cold-prone areas in Florida.			
17. Key Words (Selected by Author(s)) HCMM, Thermal-Inertia, Cold-Prone-Areas, Well-Drained-Soil, Wetlands, Soil-Temperature		18. Distribution Statement	
19. Security Classif. (of this report) UNCLASSIFIED	20. Security Classif. (of this page) UNCLASSIFIED	21. No. of Pages	22. Price*

*For sale by the Clearinghouse for Federal Scientific and Technical Information, Springfield, Virginia 22151.

Figure 2. Technical Report Standard Title Page

Table of Contents

	<u>Page</u>
Title Page	i
Acknowledgements	iii
Executive Summary	1
List of Figures	5
List of Tables	7
1.0. INTRODUCTION	9
1.1. Previous Work with GOES-IR Surface Radiance Temperature	9
1.2. HCMM System and System Objectives	10
2.0. OBJECTIVES OF THIS HCMM INVESTIGATION	10
3.0. MATERIALS AND PRODUCTS	11
3.1. HCMM Products	11
3.2. GOES Products	13
3.3. TIROS-6 Products	13
4.0. RESULTS AND FINDINGS	13
4.1. Information Assembled	13
4.2. Comparison of thermal properties from HCMM and other data sets	16
4.2.1. Comparison of 1978-79 winter max-min air temperatures with surface condi- tions which affect thermal inertia	16
4.2.2. Comparison of HCMM and GOES images using the GE Image-100 and PDP 1145 System at KSC	24
4.3. Thermal properties of organic and mineral soils in Florida	27
4.3.1. Thermal properties of organic soils in south Florida	27
4.3.2. Thermal properties of mineral soils	27
4.4. Thermal inertia analysis and interpretation	41
4.4.1. Thermal inertia classification using the GE Image-100 system	41
4.4.2. Correlation of HCMM thermal inertia with HCMM surface infrared tempera- tures	47
4.4.3. Fourier analysis of GOES temperatures	52
4.4.4. Prediction of moisture availability and thermal inertia from Carlson's model	54
4.4.5. Comparison of HCMM IR data with GOES IR data	60
4.4.6. Calculation of apparent thermal iner- tia (ATI) using temperatures from GOES satellite data	61
4.4.7. Spatial resolution and thermal prop- erties	64
4.4.8. HCMM thermal pattern of organic soil attributable to land use	68
4.4.9. Nocturnal surface temperatures, ther- mal inertia, and soil or surface properties	68
5.0. SUMMARY AND CONCLUSIONS	73
6.0. REFERENCES	74

Acknowledgements

This investigation was supported in part also by the Soil and Water Unit, Agricultural Research Service, U.S. Department of Agriculture, at Gainesville, Florida, through AgRISTARS (Early Warning/Crop Condition Assessment). Special thanks go to Gary Del Valle for computer programming support for processing HCMM data and running Carlson's models, to Pattie Everett for assistance in preparation of the final report, and to personnel at the NASA Kennedy Space Center for assistance in use of the GE Image-100 facility. We also thank personnel of the HCMM program at the Goddard Space Flight Center and their contractors for providing data and assistance, and research participants of the HCMM program for valuable discussions.

EXECUTIVE SUMMARY

Rationale and Objectives

Previous satellite remote-sensing studies have shown the presence of persistent cold-prone and warm-prone areas in Florida during winter nocturnal conditions. These differences in surface temperature patterns can determine whether or not severe damage to vegetable, fruit, and other specialty crops occurs during cold air mass frontal movements across the peninsula. Qualitatively, the surface temperature patterns appeared to be related to soils and surface moisture conditions. The surfaces with low soil moisture and/or few bodies of water in the area tended to show low nocturnal surface temperatures, whereas the surfaces with high soil moisture and/or associated bodies of water tended to show high nocturnal temperatures. Since water has a high heat capacity, surfaces with high water content tend to cool slowly relative to surfaces with low water content. Thermal inertia is a property that embodies both the heat capacity and the ability to conduct heat through the medium, i.e., high thermal inertia implies high heat capacity and/or high heat conductivity, and low thermal inertia implies either low heat capacity and/or low heat conductivity. This investigation was undertaken to determine thermal inertia features associated with the nocturnal cold- and warm-prone areas.

The objectives were to (a) determine thermal inertia of peninsular Florida surfaces from Heat Capacity Mapping Mission (HCMM) satellite thermal data obtained from day-night overpasses, and compare thermal inertia maps with maps showing relevant surface features, (b) refine patterns of winter nocturnal cold-prone areas and warm-prone areas from HCMM IR daytime and nighttime overflights, and compare these patterns with data from other satellite systems and ground-based observations, and (c) adapt a boundary-layer, energy-balance model to quantify moisture availability and thermal inertia of surface features in peninsular Florida that are associated with the observed day-night surface temperature patterns.

Scope of Work

The investigation focused on peninsular Florida, which includes the following types of surfaces: shallow lakes (e.g., Lake Okeechobee), broad rivers (e.g., St. Johns River), extensive wetlands of both organic (e.g., Everglades) and mineral (e.g., Suwanee River floodplain) soils, drained organic soil (e.g., Everglades Agricultural Area), poorly drained mineral soil (e.g., complex of the South Florida Flatwood Land Resource Area), well-drained mineral soil (e.g., complex of the Central Florida Ridge Land Resource Area), and excessively well-drained mineral soil (e.g., Ucala National Forest).

The HCMM data source was restricted to the winter of 1978-1979, since data availability was limited by satellite problems later on. Unfortunately, this winter was exceptionally cloudy and rainy over Florida, which eliminated the use of many of the overflight data. Furthermore, Florida was outside the latitude zone of the 12-hour, day-night sequences of overflight coverage by the HCMM satellite. Fortunately, we

found one time-window sufficiently cloud-free to obtain adequate data for display and analysis along the peninsula: January 29 to February 3, 1979, with a daytime overflight on January 29, a nighttime overflight on February 1, and a following daytime overflight on February 3. We used maximum and minimum temperatures from the National Climate Center data to estimate corrections for day-night temperature differences for appropriate climatological regions in Florida.

During other winters, we also used GOES IR data and NOAA-6 IR data to complement and supplement HCMM data in this investigation. Surface temperature data were also examined in view of surface moisture features at each site and antecedent moisture (i.e., antecedent rainfall) conditions.

Both computer-compatible magnetic tape data (CCT) and image data from HCMM were utilized in this analysis and report.

Results, Accomplishments, and Significance

Comparison of thermal properties from HCMM with other data sets. Selected National Climate Center (NCC) maximum and minimum temperatures for 7 zones in Florida were examined for January and February, 1979. Stations with large ranges of differences of maximum and minimum temperature were found to be located in areas generally having well-drained or excessively well-drained soils, and those with smaller differences in maximum and minimum temperatures were found to be located in areas generally having poorly drained soils, or were near wet or coastal areas. HCMM temperature difference and thermal inertia images were found to closely agree also with a general soils map of the state based on drainage properties of the soil. That is, areas where HCMM data or images showed larger day-night temperature differences or, concomitantly, smaller thermal inertia, overlaid areas with extensive well-drained to excessively well-drained soils. Likewise, areas where HCMM data showed smaller day-night temperature differences and larger thermal inertia were associated with wetter surfaces.

Direct comparison of a HCMM nighttime surface temperature image with a GOES nighttime surface temperature image showed that cold areas overlay closely. However, the HCMM IR image showed more detail than the GOES image, since it has a 0.6 x 0.6 km resolution at nadir, whereas the GOES in Florida has about a 6 x 8 km resolution.

HCMM detects similar surface patterns that GOES or surface measurements can detect, but it obviously shows more detail.

Thermal properties of organic and mineral soils. A HCMM apparent thermal inertia (ATI) image of the whole peninsula showed patterns related to surface conditions. In organic soil areas of south Florida, the areas drained for agriculture (Everglades Agricultural Area) had distinctly lower ATI values than the undrained Everglades or undrained Water Conservation Areas located on organic soils. The low ATI values corresponded closely to low nocturnal surface temperatures detected by GOES. Within the undrained Everglades, the ATI image showed that the ATI values of parts of the Everglades National Park were lower than parts of

the Water Conservation Areas. The images show the impact of water management, but at this point one could not say whether the differences from the natural conditions would be mainly due to retention of water in conservation areas, or prevention of natural flow maintaining higher water (and higher ATI) in the Everglades National Park.

Thermal properties of mineral soils in north Florida in the Suwanee River Area showed that upland areas were persistently colder at night and had lower ATI than did floodplain areas. These patterns show that surface cooling properties, not nocturnal drainage properties, predominate. An exception, which is usually at about the limits of resolution of HCMM, is found in karst depressions of the Central Florida Ridge Land Resource Area. In the spring of 1981, following severe freezes in January, 1981, we observed severe citrus tree damage in dry karst depressions, but lack of damage around karst depressions that contained water (small permanent lakes, ponds, or marshes).

Thermal inertia analysis and interpretation. The apparent thermal inertia image of February 1-3, 1979, was analyzed on the GE Image-100 at the NASA Kennedy Space Center and separated into 5 major thermal inertia classes. These classes overlaid the general soils map of Florida quite precisely, so we adopted the general soils map as a first approximation thermal inertia map of peninsular Florida. The close correspondence of ATI images to surface soil drainage classes implies that ATI could be useful in classifying wetlands in remote areas of the world.

Predicting moisture availability and thermal inertia. Carlson's energy-balance model was used to compute moisture availability and thermal inertia from three wet areas and two dry areas in north central Florida. Under these conditions, it was found that moisture availability was much more unstable than thermal inertia. Moisture availability ranged from about 0.05 to 0.96 for the driest to the wettest site. Thermal inertia ranged from about 0.085 for the wet sites to about 0.055 for the dry sites, or a difference of about $0.03 \text{ cal cm}^{-2} \text{ sec}^{-1/2} \text{ } ^\circ\text{K}^{-1}$.

Calculation of ATI from GOES data. GOES temperatures averaged 5.9°C and 5.2°C higher than the HCMM temperatures for two nights examined (January 10, 1979, and February 1, 1979, respectively). This suggests that the HCMM standard processed data may represent temperatures that are about 5.5°C too low.

The ATI in the HCMM User's Guide, 1980, was used with two GOES day-night periods (January 12-13 and January 18-19, 1981) to compute ATI for the Everglades Agricultural Area (drained organic soil with sugarcane) and for an area of excessively well-drained and well-drained soils south of Ocala, Florida. ATI was about 17.5 for this mineral soil site on both occasions, but it dropped from 36.1 to 28.5 in the organic soil area. We interpret the drop in ATI in the Everglades Agricultural Area to be due to killing of transpiring sugarcane and other vegetation leaf tissue during the first freeze event, since the day-night temperature difference changed from 19°C to 25°C . If this is the case, then evaporation from living vegetation can decrease ATI, and confound the interpretation of results. This also would imply that an energy balance model that accounts for evaporation should be used with HCMM data. Indeed, in

many applications, moisture availability and evaporation are surface parameters that are actually more useful.

Recommendations

Information gained from HCMM studies can be applied to other polar-orbiting or geosynchronous satellites that have thermal IR sensors. In many cases, GOES may be more desirable where coverage can be obtained, because the data stream is available in continuous, one-half hour intervals. In the case of many weather events, such as freezes, continuous data of a coarse resolution, such as GOES, are much more useful for both prediction of incipient freeze severity, and documentation of freeze severity, than would be 12-hour coverage from a polar-orbiting satellite. In any event, coverage at the right time every 12 hours is needed, and polar orbiters can supply this information, albeit local times and solar angles may not be very uniform.

The thermal inertia approach has value in identifying wetlands and in quantifying their condition at any given time, especially in remote and inaccessible areas. This methodology should also be useful in detecting soil moisture availability and drought severity in agricultural cropping regions, in grasslands, and perhaps even in forests. An energy balance model such as Carlson's model could probably be simplified, and certainly a better procedure for quantifying surface moisture availability and thermal inertia needs to be devised. Perhaps initializing with observed temperature data at one overpass and running to the next overpass might yield more meaningful moisture availability and thermal inertia values (although it would sacrifice whole-day evapotranspiration and other predictions).

List of Figures

- Fig. 1. Climatological regions of Florida, showing the 6 regions where rainfall data were averaged. From Climatological Data--Florida, National Climatic Center, Asheville, NC.
- Fig. 2. HCMM infrared (IR) image of lower Florida at approximately 0200 EST Feb. 1, 1979, obtained by digitizing HCMM film transparency using the Image 100 computer at Kennedy Space Center.
- Fig. 3. GOES digital image of Florida at 0200 EST, Feb. 1, 1979. The coldest area south of Lake Okeechobee (symbol Y) was blocked for comparison with the HCMM image showing the coldest area, green.
- Fig. 4. Map of lower Florida showing location of the conservation areas and Everglades National Park, and original extent of the Everglades Marsh (from Central and South Florida Flood Control District, Vol. 1, No. 5, 1972).
- Fig. 5. HCMM-derived apparent thermal inertia from daytime Feb. 3 and nighttime Feb. 1, 1979, data. Areas in south Florida were clear and were used to compare with GOES images.
- Fig. 6. GOES infrared digital data showing average temperatures for Lake Okeechobee, the Everglades Agricultural Area, and Water Conservation Areas #1, #2, and #3.
- Fig. 7. Diurnal surface temperatures obtained from GOES infrared digital data for the night of Feb. 26-27, 1980.
- Fig. 8. Diurnal surface temperatures obtained from GOES infrared digital data for nights of Jan. 11-12 and 12-13, 1981, during a severe freeze period in Florida.
- Fig. 9. GOES infrared digital map for 2100 EST, Jan. 12, 1981, showing surface temperatures within the Suwannee River area of north Florida. Coldest areas are outlined. Circles show areas where diurnal temperatures were plotted (Fig. 11). A temperature symbol scale is shown on the map. Black dots are NWS stations listed in Table 9.
- Fig. 10. HCMM-derived apparent thermal inertia image from nighttime Dec. 15 and daytime Dec. 17, 1978, data. Areas in north Florida in the Suwannee River Basin were clear although overall sky conditions were poor southward. The thermal inertia patterns of the Suwannee River Basin agreed with diurnal GOES thermal data.
- Fig. 11. GOES diurnal surface temperatures for 5 areas in the Suwannee River Basin (see Fig. 9).
- Fig. 12. General soil map of Florida, showing the 5 thermal inertia classes for Florida constructed from HCMM and GOES data (see Table 11 for description). Source: R.E. Caldwell and R.W.

Johnson, USDA-Soil Conservation Service, IFAS-Agricultural Experiment Station and Soil Science Department, revised 1982.

- Fig. 13. Five by five blocks of HCMM pixels averaged from Night IR data of Feb. 3, 1979 (A) and from Apparent Thermal Inertia data based on Feb. 1-3, 1979, day-night overflights (B), for use in relating apparent thermal inertia with nighttime surface temperatures. A...A' identifies the row of pixels listed in Table 13. See also Fig. 12.
- Fig. 14. Linear regression of thermal inertia (grey scales) and temperatures for the cross section A...A' (Fig. 13).
- Fig. 15. Fourier fit of GOES diurnal temperatures of the Everglades Agricultural Area for data from Jan. 12-13, 1981.
- Fig. 16. HCMM (AAO-281-065804) temperature difference data from Feb. 1-3, 1979. This set of data is used to obtain a day temperature (6°C was added to the temperature to correct HCMM data) to use with Carlson's model. Areas used are labeled 1, 2, and 3 (wet) and 4 and 5 (dry). The areas are also located by x's in Fig. 12.
- Fig. 17. Map showing the eight areas (1-8) where HCMM-derived surface temperatures were compared with GOES surface temperatures. ATI was calculated using ΔT obtained from GOES from Area 4 and Area 9. County lines are shown on the map.
- Fig. 18. Diurnal surface temperature (GOES) for the Everglades Agricultural Area (Area 4 in Fig. 17) for two days in January, 1981.
- Fig. 19. HCMM night IR temperatures from February 1, 1979, showing detailed (600 m resolution) land-water temperature boundaries in the Lake Apopka area.
- Fig. 20. HCMM night IR image of February 1, 1979, showing detailed (600 m resolution) land-water temperature boundaries of Newnan's Lake area in North Central Florida.
- Fig. 21. GOES IR image of Florida from February 1, 1979, 0200 EST, shows the land-water temperature boundaries for small lakes of 1 to 2 pixel area.
- Fig. 22. HCMM nighttime IR image on Jan. 15, 1979, obtained by digitizing HCMM film transparency using the Image 100 computer at Kennedy Space Center. The image illustrates thermal patterns which can be generated due to different land use.
- Fig. 23. Average low temperatures in the state during 1979-80 and 1980-81 winter seasons. Temperatures are in $^{\circ}\text{C}$. Lines are time-expansion of cold areas initiated from cold areas. Thick lines indicate average coldest conditions during midnight hours and dashed lines indicate average coldest conditions during predawn hours.

List of Tables

- Table 1. HCMM data tapes (CCT) received. The tapes are listed in the order received, according to shipment dates from GSFC.
- Table 2. Polar-orbiting NOAA-6 satellite film transparencies covering the same period as in Table 8 obtained from Environmental Data Service.
- Table 3. Dates, route, and sky conditions during transects of surface temperature (Raytek radiation thermometer), 1.5-m air temperature, and dewpoint temperature (from E. Chen and J.F. Gerber, unpublished).
- Table 4. Florida nocturnal surface temperature transects and HCMM coverage, January and February, 1979.
- Table 5. Rainfall preceding January and February, 1979, transects.
- Table 6. Average rainfall for each climatic region of Florida for the period from Dec. 16, 1980, through Jan. 16, 1981: Northwest (1); North (2); North Central (3); South Central (4); Everglades and SW Coast (5); and Lower East Coast (6). Data were from Climatological Data for Florida, National Climatic Center, Asheville, NC, Dec. 1980 and Jan. 1981.
- Table 7. NCC-NOAA climate data for selected Florida stations that show average daily temperature ranges indicative of high or low surface thermal inertia.
- Table 8. Maximum range of average daily temperature observed at climate stations within zones from NCC-NOAA climate data, 1979.
- Table 9. Maximum and minimum temperature from Jan. 12-13, 1981, for NOAA cooperative observer stations in the Suwannee River Basin of north Florida. Approximate location of the cities are indicated in Fig. 16 (black circles). Source: Climatological Data--Florida, 85, No. 1, National Climatic Center, Asheville, NC, 1981.
- Table 10. Thermal inertia classes for Florida from Feb. 1-3, 1979, Day-Night HCMM data.
- Table 11. Thermal inertia classes for Florida based on HCMM image AAO-281-6580-5 and using the Image-100 Image Analyzing System to determine areas with equal thermal inertia as defined by grey scales. Data digitized: HCMM A-AO281-06580-5 (HCMM14, File 5). Data formatted from Feb. 1 (night) and Feb. 3 (day), 1979, IR temperatures.

- Table 12. Rainfall and departures from the means for 1979 and for 1980 that determine antecedent surface moisture conditions for periods immediately before the Jan. - Feb. winter period of 1980 and 1981, respectively. Source: Climatological Data--Florida, Annual Summary, National Climatic Center, Asheville, NC 83, No. 13, 1979, and 84, No. 14, 1980.
- Table 13. HCMM thermal inertia and night IR temperatures for day-night pairs of Feb. 1-3, 1979. Data pair was taken from a cross-section in North Central Florida (Fig. 13-A and 13-B, A...A'). Temperatures are uncorrected.
- Table 14. Day-night temperature pairs for input into Carlson's model to predict thermal inertia and moisture availability.
- Table 15. Predicted thermal inertia (TI) and moisture availability (MA) for areas 1, 2, 3, 4 and 5.
- Table 16. Comparison of surface IR temperatures derived from HCMM film transparencies with GOES surface IR temperatures for 6 areas in South Florida. Temperature is in °C.
- Table 17. Values used in calculation of apparent thermal inertia (ATI) for 2 areas in Florida: Area 4, the drained organic soils of the Everglades Agricultural Area (EAA) in south Florida, and Area 9, the area classified as excessively drained and well-drained mineral soils 25 km directly south of Ocala in the west north central Florida peninsula. Data used were from Jan. 1981.

1.0. INTRODUCTION

1.1. Previous Work with GOES IR Surface Radiance Temperature

Earlier studies by Chen (1979) and Chen et al. (1981, 1982) showed that nocturnal GOES thermal imagery gave very persistent patterns of cold-prone areas throughout Peninsular Florida. These patterns have been borne out by two subsequent studies (Chen and Martsolf, 1981; Chen, Allen, and Martsolf, 1982). Transects of nocturnal air temperatures at 1.5 m measured from a moving vehicle generally showed the same temperature patterns as determined by the GOES satellite (Chen et al., 1983). However, later transects of air temperature at 1.5 m during the daytime across wetland areas and across well-drained, upland areas (from Gainesville to Cedar Key, and from Gainesville to Palatka) seemed to be uncoupled from GOES-derived surface temperature (Chen, Allen and Martsolf, 1982). (In soils terminology, well-drained may refer to good internal drainage of the soil profile as well as relief that provides good surface drainage.) The daytime GOES-derived surface temperatures were cooler than air temperatures in wetland areas and warmer than air temperatures in well-drained upland areas. Either rapid mixing resulted in the daytime 1.5-m air temperature being represented by air-mass temperature conditions, or the 1.5-m air temperature measurements were "contaminated" by road and roadside conditions, or both. Nevertheless, the close tracking of surface and 1.5-m air temperatures at night, and the decoupling of surface and 1.5-m air temperatures during the daytime seems at first unexpected, since current wisdom suggests that stably-stratified nocturnal air should effectively decouple surface and air temperatures, whereas unstably-stratified daytime air should cause close coupling of surface and air temperature. However, the findings of Chen et al. (1983) and Chen, Allen and Martsolf (1982) suggest that 1.5-m air temperature is closely coupled to the surface temperature of the nearby locale at night, and is closely coupled to the air mass temperature during the daytime.

Drained organic soil of the Everglades Agricultural Area south of Lake Okeechobee was a persistent cold-prone area identified by GOES thermal data (Chen, 1979; Chen et al., 1981). However, wet or flooded Water Conservation Areas maintained by the South Florida Water Management District were found to be considerably warmer at night during winter cold weather conditions.

In most of the mineral soil areas of Florida, patterns of cold-prone areas appeared to be related to deep, well-drained to excessively well-drained sandy soils (such as the Central Florida Ridge Land Resource Area) whereas warm areas were related to the presence of bodies of water (such as the broad downstream St. Johns River) or to poorly drained soils or wetlands areas (such as the Green Swamp area), Chen et al. (1982).

Recent antecedent rainfall appears to reduce the winter nocturnal cold tendency of well-drained soils (Chen et al., 1982), whereas long-term drought tends to increase the winter nocturnal cold tendency of usually high water table soils that have drained or had soil water removed by evapotranspiration (Chen, Allen and Martsolf, 1982).

1.2. HCMM System and System Objectives

The HCMM satellite was launched on April 26, 1978, into a near-polar orbit with equatorial crossing times at near 1430 and 0230 local times. In the latitude band of about 35° to 85°, 12-hour day-night overpass intervals were available. However, in the 22°N latitude to 35°N latitude, day-night sequence images were available at only 36-hour intervals. This problem was recognized in the project proposal so that enough HCMM products were planned for request from NASA so that paired day-night sequences under similar weather conditions could be selected for analysis. The project proposal also called for use of other satellite products, such as GOES, for supplying additional and supplemental information for missing data sequences or different years.

Earlier uses of HCMM data have been to evaluate water surface temperatures and motion or mixing patterns, geologic formations, snow cover, evapotranspiration and land cover patterns. Perhaps one of the most analytic applications was the use of HCMM day-night overpass sequences of surface temperature patterns to compute surface thermal inertia and surface moisture availability at several test sites within the U.S.A. (Carlson et al., 1981).

2.0. OBJECTIVES OF THIS HCMM INVESTIGATION

The rationale and objectives of this particular investigation were derived from several sources, first being the overall objectives of the HCMM program. Second, findings from previous work in Florida with GOES IR data provided background for ideas that needed to be investigated. Third, early HCMM investigations elucidated further applications opportunities.

The specific objectives of this report of HCMM investigations are:

- (A) Determine Thermal Inertia of Peninsular Florida surfaces from winter Heat Capacity Mapping Mission (HCMM) thermal data under a range of surface and soil moisture conditions, and develop maps that compare thermal inertia with relevant surface features.
- (B) Refine patterns of winter nocturnal cold-prone areas and warm-prone areas from both nighttime and daytime overflights and compare these patterns with other data from other satellite systems.
- (C) Adapt a boundary-layer, energy-balance model (Carlson's model) to determine patterns of moisture availability and thermal inertia from HCMM data over different surface features in Florida, and show how nighttime minimum surface temperature can be predicted from daytime surface temperature and thermal inertia information.

3.0. MATERIALS AND PRODUCTS

3.1. HCMM products

The products available to HCMM users were computer-compatible tapes and negative or print images of daytime visible, daytime IR, or nighttime IR data. Also, rectified day-night temperature differences or apparent thermal inertia could be obtained as negatives, prints, and computer-compatible magnetic tapes. We obtained these types of data for the winter of 1978-79 (Table 1).

The lack of 12-hour, day-night sequence of HCMM satellite overflights in Florida, and the lack of clear periods in Florida during HCMM overflights during the winter of 1978-79 were two major uncontrollable problems in identification and selection of suitable data for analysis. Lack of "user-friendly" documentation on computer-compatible tapes, lapse of time between order and receipt of products, and a few defective or missing products were minor controllable problems. All problems contributed to delays in completing this HCMM investigation task.

(A) Lack of 12-hour, day-night sequence of HCMM satellite overflight in Florida latitudes

This problem was detailed in the First Quarterly Report (HCMM Data Investigation HFO-002, Contract NAS5-24653, March 16 to June 15, 1981). We solved this problem partially by calculating sequential daily maximum and minimum temperatures from climatological data (Climatological Data for Florida, Asheville, NC, NOAA, USDC) averaged over the region of Florida where satellite data were to be analyzed. The daytime maximum and nighttime minimum climatological temperatures were used to adjust the 36-hour (or greater) overflight interval day and night temperatures of HCMM so that a reasonable pair of temperature data were obtained. This procedure will be discussed in more detail in a later section. Also, GOES IR temperatures were used extensively to supplement and calibrate (or corroborate) the HCMM data.

(B) Lack of clear periods during 1978-79 HCMM overflights

The winter of 1978-79 had more cloudy periods than usual. Therefore, it was difficult to find clear day and night pairs of images of HCMM data that were reasonably close together in time, and which represented cold weather conditions. This problem was compounded by the lack of 12-hour, day-night overpass sequences. From the available HCMM data, we selected the period from January 29 to February 3, 1979, as the best period for data analysis. This period gave a good nighttime overpass on February 1, sandwiched between good daytime overpasses on January 29 and February 3. This period coupled well with GOES IR data which were available to us, and represented a relatively moist period, but a period with clear-sky conditions during HCMM satellite overpasses. GOES IR temperatures from 1980-81 were used to represent a dry period. GOES 12-hour, day-night temperatures were used in place of HCMM data in this latter period.

Table 1. HCMM data tapes (CCT) received. The tapes are listed in the order received, according to shipment dates from GSFC.

Date Received	Scene ID		Local Tape Name	Comments
	AAO-	Files		
18 Sept 1981	259-065703	1-4	HCMM1	
	265-070703	5-8	"	
	267-182801,2	9-15	"	
1 Oct 1981	233-07130,P	--	HCMM2	
	233-07130,P	--	HCMM3	
	278-183506,7,8	--	HCMM4	
	278-183506,7,8	--	HCMM5	
	278-183506,7,8	--	HCMM6	
12 Oct 1981	265-065806,7,8	--	HCMM7	Tape is bad, data no longer available
	265-065806,7,8	--	HCMM8	
	265-065806,7,8	--	HCMM9	
30 Oct 1981	281-070403	1-7	HCMM10	
	283-183001,2	8-14	"	
	264-064903	15-18	HCMM11	
	233-071303	19-22	"	
	262-183701,2	1-7	"	
	235-183611,1	8-14	"	
	278-183501,2	1,7	HCMM12	Not readable
	278-183601,1	8-13	"	
9 Nov 1981	281-06580P(20/3)	1-8	HCMM13	
	281-06580P(30/3)	1-6	HCMM14	
	281-06580P(10/3)	1-6	HCMM15	
10 Nov 1981	259-064806	--	HCMM16	
	259-06480	--	HCMM17	
	259-064804,5,6,7,8	--	"	
12 Nov 1981	262-18320	--	HCMM18	First record bad, no readable directory Continuation of 18? Empty
	262-18320	--	HCMM19	
	262-18320	--	HCMM20	
3 Mar 1982	283-132801,2	1-7	HCMM21	
	233-071303	1-4	HCMM22	Replacement for a previous bad tape
12 July 1982	278-183501,2	1-7	HCMM32	Replacement tape for previous bad tape
	281-065803	8-11	"	
	259-064803	12-15	"	
	262-183201,2	16-22	"	

(C) HCMM tapes documentation

The HCMM tapes lacked "user-friendly" information on the tapes as they were sent to us. The label on each tape contained minimal information on scene ID. Sometimes a scene that was not completed on one tape was put on another tape without clear documentation. When an attempt was made to read such a tape, errors were encountered because no header information was found. After repeated failures, each tape was dumped and the content examined to obtain each file contained in each tape. This process was time-consuming and expensive. One tape was not readable. The first record of one tape was bad and there was no readable tape directory. One tape was empty. A total of 23 tapes were received (Table 1). NASA-Goddard personnel and contractor personnel provided assistance and replacement tapes.

3.2. GOES Products

GOES infrared digital printouts of the Florida sector from the Satellite Freeze Forecast System (SFFS), J.D. Martsof, Principal Investigator, were used extensively to supplement the HCMM data. Data usually covered the nighttime period of January and February of each year (1977-1981). Average low temperature maps (1979-80, 1980-81 winters) developed from GOES for another project (Chen and Martsof, 1982) were also used as a basis for qualitatively extending thermal inertia obtained from HCMM to the entire state of Florida.

3.3. TIROS-6 Products

NOAA-6 positive film transparencies that were obtained in the winter of 1980-81 are shown in Table 2. Day-night sequence of NOAA-6 frames for the 3 periods classified as wet-cool, intermediate dry-cool and dry-cold were selected from the film transparencies and digital magnetic tapes were ordered.

4.0. RESULTS AND FINDINGS

4.1. Information assembled

In addition to HCMM, GOES, and NOAA-6 satellite products, other data, such as National Climatic Center cooperative-observer temperature and rainfall data, and surface transect observations from a moving vehicle, were assembled. These data were tabulated for comparisons, analyses, and interpretations that are discussed in later sections.

During January and February, 1979, surface transects were made for 11 overnight periods in Florida during cold night conditions by Ellen Chen and J.F. Gerber (Table 3). The data collected included radiation surface temperature, air temperature, dewpoint temperature, windspeed, and sky condition observations.

Table 2. Polar-orbiting NOAA-6 satellite film transparencies obtained from Environmental Data Service, covering the same period as in Table 4.

Date	Time	Orbit Number	Weather Condition
Dec. 17, 1980	352:01:08:32	7655	wet, cool
Dec. 17, 1980 ^{1/}	352:13:29:22	7662	
Dec. 18, 1980 ^{1/}	352:23:10:22	7669	
Dec. 18, 1980	353:13:08:32	7676	
Dec. 31, 1980	366:00:53:20	7854	intermediate
Dec. 31, 1980 ^{1/}	366:13:16:01	7861	dry, cool
Jan. 1, 1981 ^{1/}	001:12:56:02	7875	
Jan. 3, 1981 ^{1/}	003:13:49:16	7904	
Jan. 10, 1981	010:00:31:30	7996	dry, cool
Jan. 10, 1981	010:12:55:02	8003	
Jan. 12, 1981 ^{1/}	012:13:48:11	8032	
Jan. 13, 1981 ^{1/}	012:23:33:28	8039	
Jan. 13, 1981	013:13:26:46	8046	

^{1/} Indicated digital magnetic tapes ordered.

Table 3. Dates, route, and sky condition during transects of surface temperature (Raytek radiation thermometer), 1.5-m air temperature, and dewpoint (from E. Chen and J.F. Gerber, unpublished).

Number	Date	State Road	Sky Condition	Satellite Maps	Number of Trucks ^{3/}
1	Jan. 24-25, 1979	50	cirrus	yes	2
2	Jan. 8-9, 1979	24	clear	incomplete ^{2/}	1
3	Jan. 9-10, 1979	50	clear	yes	1
4	Jan. 14-15, 1979	50	cirrus	incomplete ^{2/}	2
5	Jan. 22-23, 1979	24	cirrus	yes	1
6	Jan. 24-25, 1979	24	cirrus	yes	1
7	Feb. 1-2, 1979	40	clouded out	yes	2
8	Feb. 8-9, 1979	40	clouded out	yes	1
9	Feb. 10-11, 1979	40	clear	yes ^{2/}	1
10	Feb. 19-20, 1979	40	clear	yes ^{2/}	2
11	Feb. 27-28, 1979	27	low clouds	yes ^{2/}	2
		80	clear, patchy fog		

^{1/} Sky condition refers to sky over the transect region

^{2/} From NOAA/EDS; hours available: 0, 3, 6, 9, 12 GMT (19, 22, 1, 4, 7 EST)

^{3/} Most of the transects were from: 10 to 11:30 PM EST, 1 to 2:30 PM EST, and 5 to 6:00 PM EST

Periods of no rainfall and antecedent rainfall during January and February, 1979, shown in Table 4 and Table 5 helped to determine conditions for wet and dry fronts, and hence, wet and dry periods. Nine of the 11 nocturnal transect periods had HCMM overpasses before, during, or after the transects that were in overlapping range to give surface coverage. The February 8-9 period had daytime coverage both before and after. Six potential day overflights and 4 potential night overflights were available. However, HCMM data for daytime overflights were missing on January 8, February 8, and February 9, 1979.

GOES maps were also available during the transect periods listed in Tables 3 and 4. Rainfall conditions preceding the cold fronts (cold nights) are listed in Table 5. From the array of HCMM coverage, GOES maps and transect periods, rainfall conditions, and cloud problems, we selected suitable periods to determine the effects of surface thermal inertia on predicting nocturnal low temperatures. Several data sources were needed to obtain adequate surface temperature coverage of the state because of the prevalence of clouds in some part of the state in many of the HCMM scenes.

NOAA-6, polar-orbiting satellite infrared (10.5 to 12.6 microns) digital magnetic tape data for December, 1980, and January, 1981 (Table 2), were selected according to rainfall information from climatological data (Table 6). Geostationary satellite (GOES) infrared digital images showed that most of peninsular Florida was clear during periods of no rainfall on December 17-18, 1980, the period from the night of December 31, 1980, through the morning of January 3, 1981, the night of January 10, through the morning of January 13, 1981, and finally, from January 17-19, 1981. The period of December 17-18 was classified wet and cool (Table 2), because an average of 0.63 cm (0.25 inches) or more of rain fell in each climatological region of peninsular Florida (Fig. 1) during the period of December 16-17 (Table 4). Nighttime temperatures were about 3-5°C. The clear period from December 31, 1980, to January 3, 1981, was classified intermediate dry and cool. Rainfall for the 4 days (December 28-31) preceding the clear period was from no rainfall to trace amounts (Table 6). Nighttime temperatures in the peninsula were around 0°C and below. The period of January 10-13, 1981, was classified as dry and cold. Table 6 showed that there was negligible rainfall in peninsular Florida during the period of January 4-9, 1981, which enhanced the antecedent dry condition of the state. Nighttime temperatures were below freezing for the entire state, with minimum temperatures of -10 to -11°C in northern Florida and parts of peninsular Florida.

4.2. Comparison of thermal properties from HCMM and other data sets

4.2.1. Comparison of 1978-79 winter max-min air temperatures with surface conditions which affect thermal inertia

Selected National Climate Center (NCC) maximum and minimum temperatures for 7 zones in Florida (Northwest, North, North Central, South Central, Everglades and S.W. Coast, Lower East Coast, and Keys; NCC-NOAA, 1979) were examined for January and February, 1979. The monthly

Table 6. Average rainfall for each climatic region of Florida for the period from December 16, 1980, through January 16, 1981: Northwest (1), North (2), North Central (3), South Central (4), Everglades and SW Coast (5), and Lower East Coast (6). Data were from Climatological Data for Florida, National Climatic Center, Asheville, NC, December, 1980, and January, 1981.

Date	No. of Stations	Climatic Regions					
		(1)	(2)	(3)	(4)	(5)	(6)
		15	20	13	28	14	11
1980							
Dec. 16		.23	.11	.18	.15	.04	.04
17		.04	.13	.09	.37	.49	.21
22		.06	.02	.21	.30	.06	.01
23		.09	.14 ^{1/}	.09 ^{2/}	.09	.12	.37
24		.06	Tr ^{1/}	NR ^{2/}	.01	.10	.15
25		.10	.09	Tr	.03	.02	.01
26		.01	Tr	NR	.01	Tr	.02
27		.02	Tr	NR	.01	NR	NR
28		Tr	.01	Tr	Tr	NR	Tr
29		.06	.05	Tr	Tr	Tr	.03
30		Tr	Tr	Tr	Tr	Tr	Tr
31		NR	NR	NR	Tr	NR	NR
1981							
Jan. 7		.56	.40	.09	.01	Tr	Tr
8		NR	.03	.02	.01	Tr	Tr
14		.01	Tr	Tr	NR	NR	NR
15		.04	.11	.06	Tr	NR	NR
16		NR	Tr	Tr	Tr	.01	.02

^{1/} Tr = Trace
^{2/} NR = No Rainfall

Table 4. Florida nocturnal surface temperature transects and HCMM coverage, January and February, 1979.

Nocturnal Surface Temperature Transects (1979)	HCMM Coverage					GOES/SMS Maps	Sky Cond.	Rain ^{1/}
	Date	Cycle Number	Reference Day Number	Day or Night	Before or After Transect			
Jan. 3-4	Orlando/KSC	None					cirrus	Jan. 2-3
Jan. 8-9	Cedar Key/Archer	Jan. 8	17	0/16	day	before	clear	incompl. Jan. 8
Jan. 9-10	Bayport/Groveland	Jan. 10	17	2	night	during	clear	yes Jan. 8
Jan. 14-15	Bayport/Groveland	Jan. 15	17	7	night	during	cirrus	incompl. Jan. 13
Jan. 22-23	Cedar Key/Archer	Jan. 23	17	15	day	after	cirrus	yes Jan. 21
Jan. 24-25	Cedar Key/Archer	Jan. 24	18	0/16	day	before	cirrus	yes Jan. 24
Feb. 1-2	Yankeetown/1-75	None					cloud	yes Jan. 31
Feb. 8-9	Yankeetown/1-75	Feb. 8	18	15	day	before	cloud	yes Feb. 7-8
Feb. 8-9	Yankeetown/1-75	Feb. 9	19	0/16	day	after	cloud	yes Feb. 7-8
Feb. 10-11	Gulfport/SR 484	Feb. 11	19	2	night	during	clear	yes Feb. 7-8
Feb. 19-20	Ormond Beach/Ocala	Feb. 19	19	10	day	before	clear	yes Feb. 19
Feb. 27-28	South Bay/Homestead	Feb. 28	20	3	night	during	to cloud	yes Feb. 25-26
Feb. 27-28	Ft. Myers/Clewiston	Feb. 28	20	3	night	during	clear, patchy fog	yes Feb. 25-26

^{1/} See Table 5 for rainfall preceding transects.

Table 5. Rainfall preceding transects in January and February, 1979.^{1,2/}

Jan. 2-3	Generally greater than 1 inch throughout the state, mostly on Jan. 2, with some on Jan. 3.
Jan. 8-9	Almost all rain on Jan. 8. Generally less than 0.5 inch.
Jan. 9-10	Almost all rain on Jan. 8. Generally less than 0.5 inch.
Jan. 14-15	Almost all rain on Jan. 13, small amount on Jan. 14. Generally less than 1.0 inch.
Jan. 22-23	Almost all rain on Jan. 21. Generally greater than 1.0 inch N, less than 1 inch NC and SC.
Jan. 24-25	All rain on Jan. 24, generally greater than 1 inch.
Feb. 1-2	Almost all rain on Feb. 8, locally heavy, generally less than 0.5 inch.
Feb. 10-11	No rain since Feb. 8, locally heavy, generally less than 0.5 inch.
Feb. 19-20	Light rain in north section, generally less than .25 inch.
Feb. 27-28	Most rain on February 25, variable, but generally greater than 1 inch. Variable rain on Feb. 26, generally less than 0.5 inch.

^{1/} Monthly rainfall was about 7 inches for January for the North, North Central, and South Central parts of the peninsula. This amount is over twice the normal.

^{2/} February rainfall was about 3, 2, and 1.5 inches in the North, North Central, and South Central zones.

average minimum air temperature was subtracted from the monthly average maximum air temperature for each selected station to give the average daily temperature range. A large range indicates low surface thermal inertia, and a small range indicates high surface thermal inertia. These ranges of temperature were tabulated in descending order for specific stations within each zone in Table 7. The maximum range of average daily temperature averaged across all stations within each climate zone are given in Table 8. Specific stations within each zone are discussed below.

Northwest Zone (1). Station Fountain shows low thermal inertia soil effects, whereas Apalachicola shows the moderating high thermal inertia effects of the Apalachicola River wetlands and perhaps Apalachicola Bay.

North Zone (2). Stations High Springs, Cross City, and Live Oak show large average daily temperature ranges indicative of well-drained soils with low thermal inertia. Lake City, only about 25 miles from Live Oak, shows high thermal inertia associated with poorer-drained soil. Hastings and Federal Point show higher thermal inertia associated with the St. John's River. This area was identified as a warm area by Chen et al. (1979).

North Central Zone (3). Station Ocala is in the middle of a cold-prone area extending down the middle of the state. Alexander Springs is near the edge of the Ocala National Forest, an area with excessively drained soils. Inverness represents a strip of land on the west side of the state north of Tampa Bay that has been shown to be cold-prone. DeLand is on an "island" of cold-prone soils. All these stations are on well-drained soils. Sanford and Clermont stations have smaller temperature ranges caused by wetlands and lakes, respectively. Clermont represents the warmer area of the central lake region of Florida.

South Central Zone (4). Stations Bartow, Archbold, and Lake Alfred are in well-drained soil areas and have large average daily temperature ranges. St. Petersburg shows the very strong moderating effect of Tampa Bay and the Gulf of Mexico. Okeechobee Hurricane Gate #6 Station is adjacent to the north side of Lake Okeechobee, and shows the lake moderation effect on the temperature range even though the site is on the up-wind side of the lake when northerly flows occur. Fellsmere shows the effects of a wetlands region, near the St. John's marsh in the headwaters region of the St. John's River.

Everglades and S.W. Coast Zone (5). Station Belle Glade is just south of Lake Okeechobee located on drained organic soil, but the intermediate value of average daily temperature range suggests that the low thermal inertia of drained organic soil is modified by proximity to the lake. Tamiami Trail shows the high thermal inertia of the undrained Everglades. There is no NCC reporting station within the drained Everglades that would give the sharp definition of this cold-prone area shown by Chen et al. (1979) from GOES data. LaBelle is in an agricultural area of somewhat poorly drained sandy soils (high water tables), but it had 5.64 inches of rain in January and only 0.46 inches of rain

Table 7. NCC-NOAA Climate data for selected Florida Stations that show average daily temperature ranges indicative of high or low surface thermal inertia.

Zone	Station	Range (°F)		Surface Conditions
		Jan.	Feb.	
1	Fountain 3 SSE	27.6	28.0	well drained
	Apalachicola	19.8	18.8	wetlands/bay
2	High Springs	31.6	(28.3)	well drained
	Cross City	27.5	25.9	well drained
	Live Oak	25.8	25.2	well drained
	Lake City	22.7	21.5	poor drained
	Hastings	22.8	21.1	St. Johns River
	Federal Point	21.1	20.6	St. Johns River
3	Ocala	27.5	29.5	well drained
	DeLand	28.6	28.6	well drained
	Alexander Springs	30.0	27.1	Ocala Mat. For.
	Inverness	27.3	27.6	well drained
	Sanford	23.7	22.4	wetlands
	Clermont	21.5	23.8	lakes
4	Bartow	28.7	28.3	well drained
	Archbold	26.5	27.7	well drained
	Lake Alfred	26.2	27.1	well drained
	Fellsmere	22.3	23.0	wetlands
	Okeechobee	21.0	19.2	Lake Okeechobee
	St. Petersburg	16.8	17.5	bay
5	La Belle	23.9	28.2	high water table ^{1/}
	Tamiami Trail	22.2	--	Everglades,
	Belle Glade	20.8	22.5	muck/lake ^{2/}
6	Loxahatchee	23.4	27.4	mixed ^{3/}
	Miami Beach	11.7	11.5	island

^{1/} See text for January vs. February rain effect.

^{2/} The drained organic soil effect is probably masked by proximity to Lake Okeechobee.

^{3/} Confounding effects of January vs. February rainfall and proximity to drained organic soil, undrained water conservation areas, and well drained sandy soil.

Table 8. Maximum range of average daily temperature observed at climate stations within zones from NCC-NOAA climate data, 1979.

Zone	Month	Max. Range (°F)	Min. Range (°F)	Difference
1	Jan.	27.6	19.8 ^{1/}	9.5
	Feb.	28.0	18.3 ^{1/}	9.7
2	Jan.	31.6	21.1 ^{2/}	11.5
	Feb.	(28.3)	20.6 ^{3/}	8.9
3	Jan.	30.0	21.5	8.5
	Feb.	29.5	22.4 ^{4/}	7.1
4	Jan.	28.7	20.1 ^{5/}	8.6
	Feb.	28.3	19.2 ^{5/}	9.1
5	Jan.	23.9	19.6	4.3
	Feb.	28.2	20.6	8.6
6	Jan.	23.4	18.9 ^{6/}	4.5
	Feb.	27.4	17.8 ^{6/}	9.6

^{1/} excludes Pensacola

^{2/} excludes Jacksonville Beach

^{3/} excludes Jacksonville Beach and Fernandina Beach

^{4/} excludes Daytona Beach

^{5/} excludes St. Petersburg

^{6/} excludes Miami Beach and Miami

in February. Thus, it showed higher thermal inertia properties in January than in February.

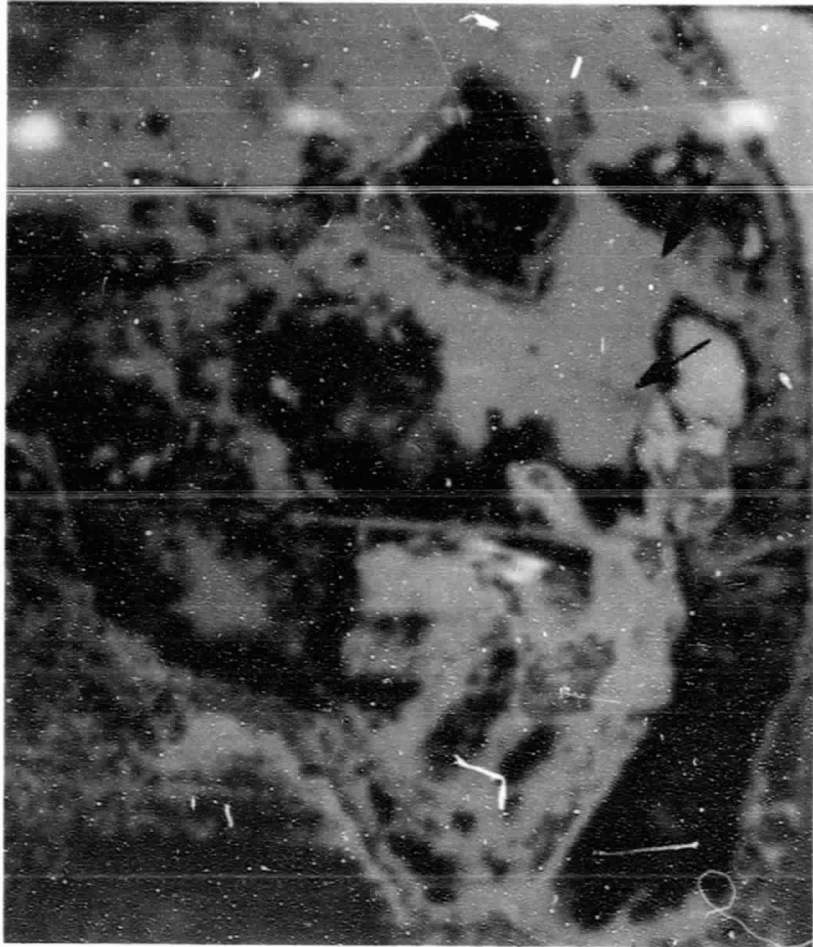
Lower East Coast Zone (6). Station Miami Beach shows the extreme case of effects of an island surrounded by water. Loxahatchee is near the boundary between deep sands, drained organic soil, and an undrained organic soil water conservation area. It showed evidence of a higher thermal inertia during January than during February.

There is some evidence in the climate records that some stations had a much larger increase in the average daily temperature range in February, 1979 (a dry month) than in January, 1979 (a wet month). In the North Zone, Stations Gainesville and Usher Tower increased by +2.7 and +2.1°F, respectively (neither of these two stations are listed in Table 7). Also, there was a general increase in the average daily temperature range in the South Central (4), Everglades and S.W. Coast (5), and Lower East Coast (6) regions due to the significantly lower February rainfall (Table 8). Furthermore, 18 out of 25 Stations showed this effect. Of the 18 stations not near a shoreline, 16 showed the effect of higher ranges of average daily maximum and minimum temperatures during the dry February than during the wet January.

These air temperature data show wide ranges at different stations throughout the state. Surface temperature ranges would probably be even wider, because low thermal inertia surfaces would rise higher in temperature during daytime solar loading, and drop lower during nocturnal radiative cooling. Nevertheless, these air temperature data show clearly that thermal properties of the underlying surfaces vary considerably. These differences are due largely to thermal inertia mediated through water content of the surfaces (soils, or complexes of soils, wetlands, and water bodies). The stations with the largest temperature ranges generally had both higher than average maxima and lower than average minima within a climate zone. The sparse NCC climate station measurements such as these can be used to help verify satellite observations.

4.2.2. Comparison of HCMM and GOES Images using the GE Image-100 and PDP 1145 Systems at KSC

In order to determine the feasibility of using GOES images to supplement HCMM data analysis, HCMM film transparencies were digitized by using the Image-100 system and one resultant image (Fig. 2) was compared with GOES thermal patterns. Images compared were for 0200 EST, February 1, 1979. Fig. 2 showed a HCMM nighttime temperature image digitized into eight themes (represented by colors) after eliminating grey scales not found on the surface of Florida. The coldest areas in the HCMM scene are indicated by arrows. They corresponded well with surface temperature patterns of the GOES coldest pixels (x, y) pointed out in Fig. 3, which lie in the cold-prone Everglades Agricultural Area (Chen, 1979; Chen et al., 1979). Because of different levels of temperature slicing, the high resolution HCMM image (Fig. 2) showed small clusters of both cold areas and warm areas, whereas the low resolution GOES image showed larger extended areas of cold or warm pixels. However, the important point is that the shape of the thermal patterns were similar.



Key

1. Green (coldest)
2. Orange
3. Dark blue
4. Yellow
5. Magenta
6. Light blue
7. Black
8. White (warmest)

Fig. 2. HCMM infrared (IR) image of lower Florida at approximately 0200 EST Feb. 1, 1979, obtained by digitizing HCMM film transparency using the Image 100 computer at Kennedy Space Center. Arrows show coldest areas.

GOES IR digital map of Florida
0200 EST, Feb. 1, 1979

HCMM	GOES	
	Temp (°C)	Symbol
1. Green	4.3 - 4.8	Y @
2. Orange	5.3 - 6.8	A B C D
3. Blue, Dk	7.3 - 8.3	9 \$.
4. Yellow	8.8 - 10.3	* 6 7 8
5. Magenta	10.8 - 11.3	5 %
6. Blue, Lt	11.8 - 12.3	4 3
7. Black	12.8 - 13.3	2
8. White	> 13.8	

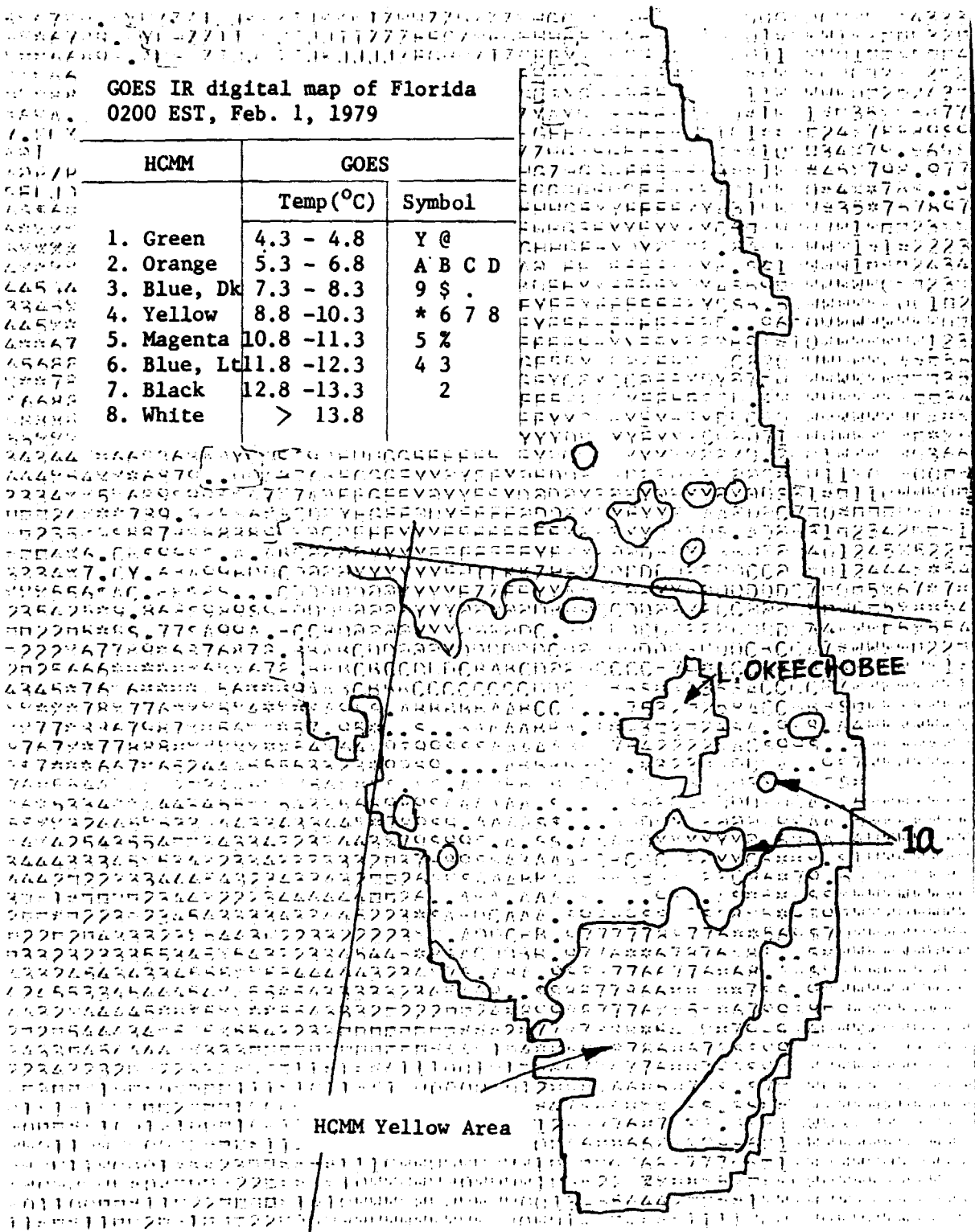


Fig. 3. GOES digital image of Florida at 0200 EST, Feb. 1, 1979. The coldest area south of Lake Okeechobee (symbol Y) was blocked for comparison with the HCMM image showing the coldest area, green.

4.3. Thermal properties of organic and mineral soils in Florida

4.3.1. Thermal properties of organic soils in south Florida

From Lake Okeechobee southward, the topography of Florida is flat and lies at low elevations. A wide strip from Lake Okeechobee to Florida Bay consists of organic soils (Fig. 4). An area south of Lake Okeechobee is drained and used for agriculture; it is called the Everglades Agricultural Area. Large canals extend from Lake Okeechobee to the southeast coast. Three Water Conservation Areas are located in organic soil to the southeast and south of the Everglades Agricultural Area. The Everglades National Park is located south of these Water Conservation Areas onward to Florida Bay.

HCMM apparent thermal inertias and temperature differences derived from daytime February 3, 1979, data and nighttime February 1, 1979, data (Fig. 5) for south Florida showed similar patterns to GOES-detected surface temperatures of the same area and for approximately the same time (Fig. 6). The HCMM-derived data showed distinct boundaries between the drained organic soil of the Everglades Agricultural Area and the undrained organic soil of the Water Conservation Areas #1, #2, and #3, managed by the South Florida Water Management District (Fig. 4), as well as between the Water Conservation Areas and the southeast coastal land area. Differences among the three Water Conservation Areas are present but they are less distinct. The GOES surface pattern for 0100 EST, January 29, 1979, showed a difference of 5-6°C between the Everglades Agricultural Area and the Water Conservation Areas, and a difference of only 1-2°C among the three Water Conservation Areas. Data from February 1, 1979, showed generally equivalent differences (Fig. 6). The HCMM-calculated difference in apparent thermal inertia indicates a difference in temperatures and thermal properties of the surface. The region has the same organic soil base, but a different surface water content due to differences in land use and water management. Differences in surface water content contributed to the difference in thermal inertia. Atmospheric conditions would affect the regions equally because of the proximity of the areas. We could not accurately quantify the apparent thermal inertia from the HCMM prints that were received, but the patterns of the HCMM-derived apparent thermal inertias for the areas are supported by the GOES surface thermal patterns (Fig. 6) and the GOES diurnal surface temperature wave for different dates (Figs. 7 and 8). The diurnal surface temperature range of the Everglades Agricultural Area is the largest (Fig. 7) which corresponds with the light gray scale of the apparent thermal inertia image (Fig. 5), whereas the smaller diurnal temperature ranges of the Water Conservation Areas corresponds closely to the darker gray scales in Fig. 6.

4.3.2. Thermal properties of mineral soils

The Suwannee River (Fig. 9) flows through an extensive area of well-drained sandy soil in north Florida. GOES surface temperatures indicated that the area appeared persistently colder than surrounding areas (Fig. 9). The colder areas corresponded closely to well-drained sandy soils and to LANDSAT-identified cleared areas. HCMM apparent thermal inertia for the area (Fig. 5 or Fig. 10, circled area) showed the

ORIGINAL PAGE IS
OF POOR QUALITY

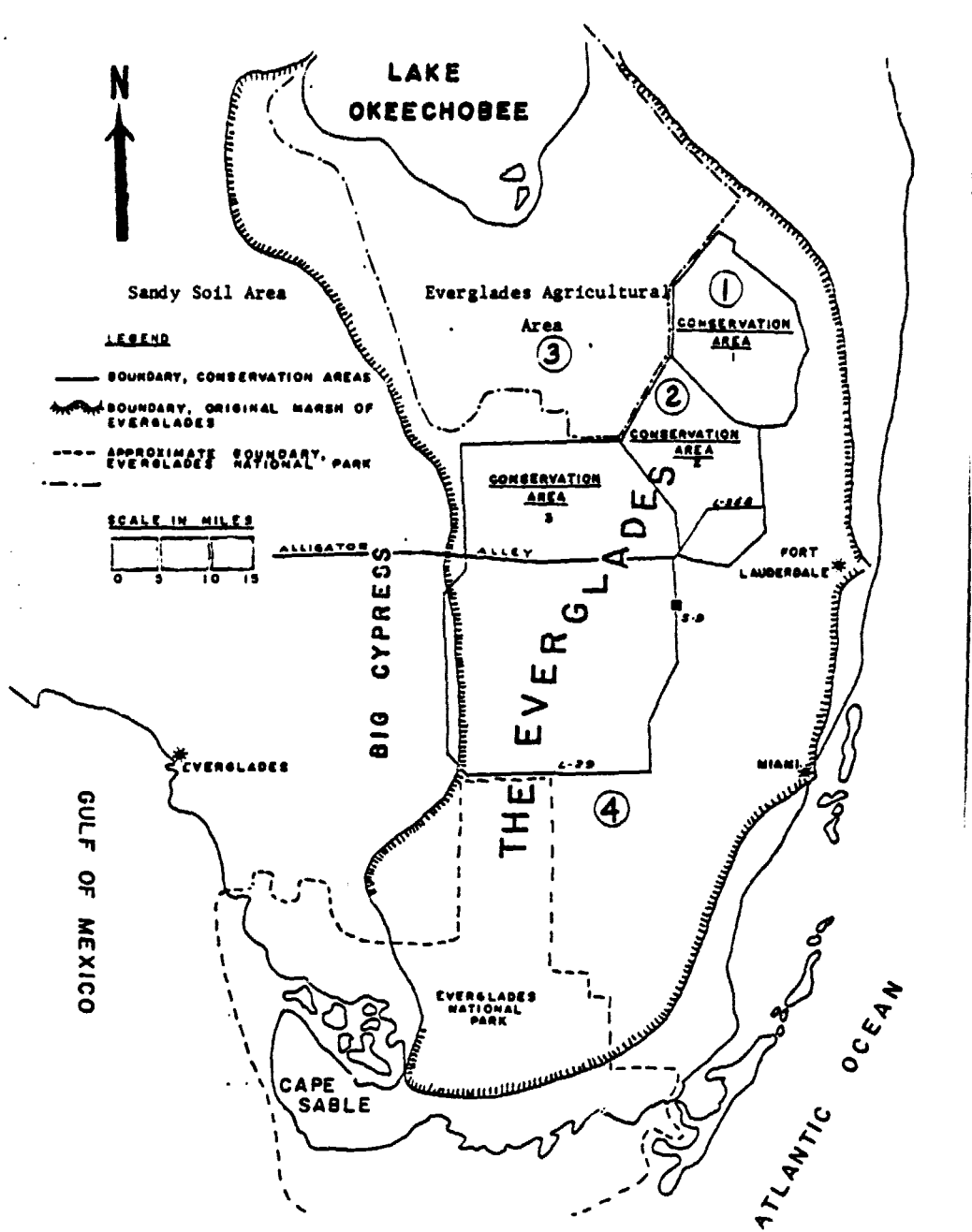


Fig. 4. Map of lower Florida showing location of the conservation areas and Everglades National Park, and original extent of the Everglades Marsh (from Central and South Florida Flood Control District, Vol 1, No. 5, 1972).

Fig. 5. HCMM-derived apparent thermal inertia from daytime Feb. 3 and nighttime Feb. 1, 1979, data. Areas in south Florida were clear and were used to compare with GOES images.

PRECEDING PAGE BLANK NOT FILMED



ORIGINAL PAGE IS
OF POOR QUALITY

0080* 0060* 0070* 0080* 0090* 0100* 0110* 0120* 0130* 0140*
83 FEB 79 E 1 38-17 W083 42 THE KPHL J N 1344 1725 H 1 0 NHSP #CM H H #0281 06580-5 0110*



J-1

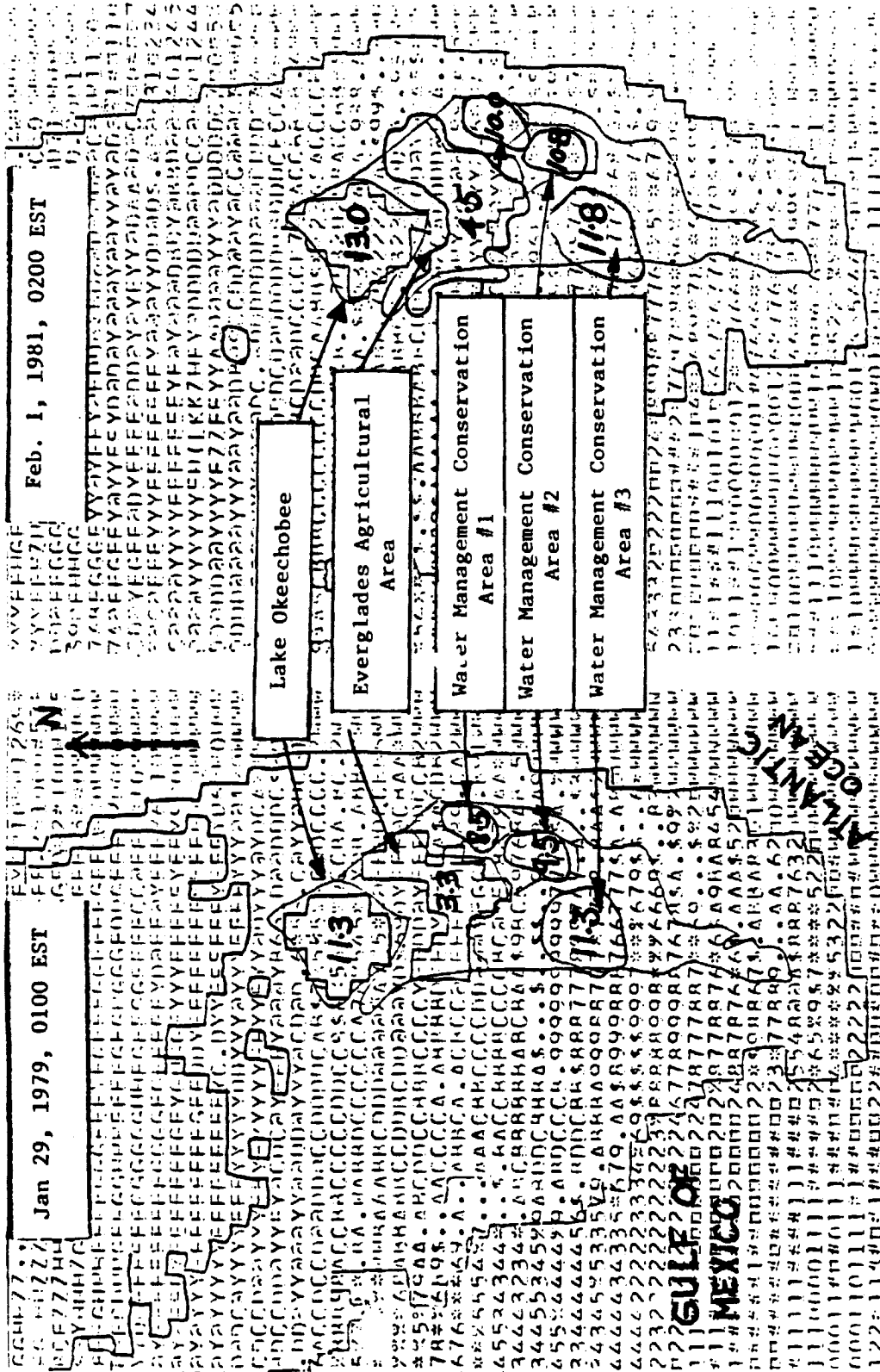


Fig. 6. GOES infrared digital data showing average temperatures for Lake Okeechobee, the Everglades Agricultural Area, Water Management Conservation Areas #1, #2, and #3.

PRECEDING PAGE BLANK NOT FILMED

ORIGINAL PAGE IS
OF POOR QUALITY

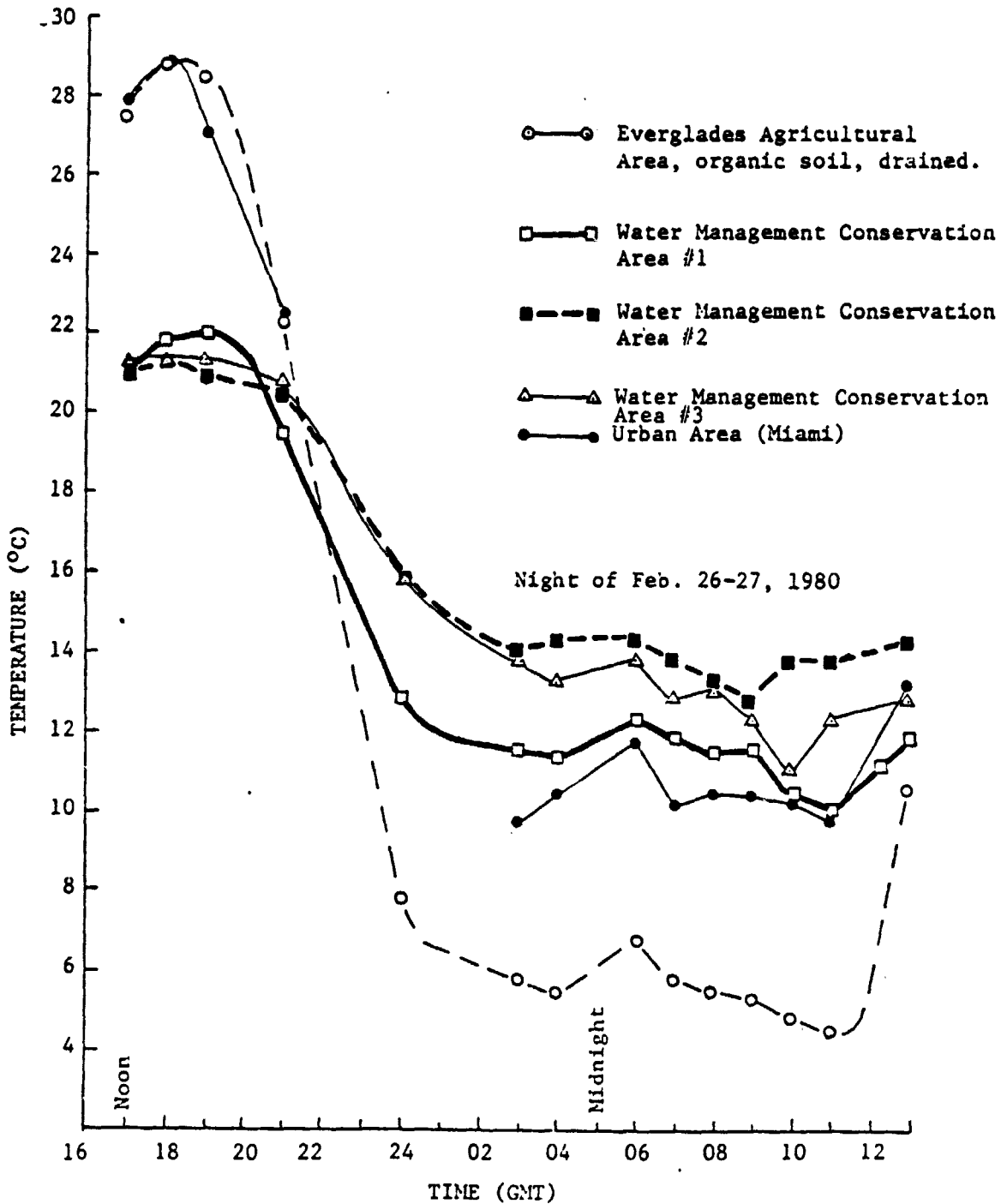


Fig. 7. Diurnal surface temperatures obtained from GOES infrared digital data from the night of Feb. 26-27, 1980.

ORIGINAL PAGE 18
OF POOR QUALITY

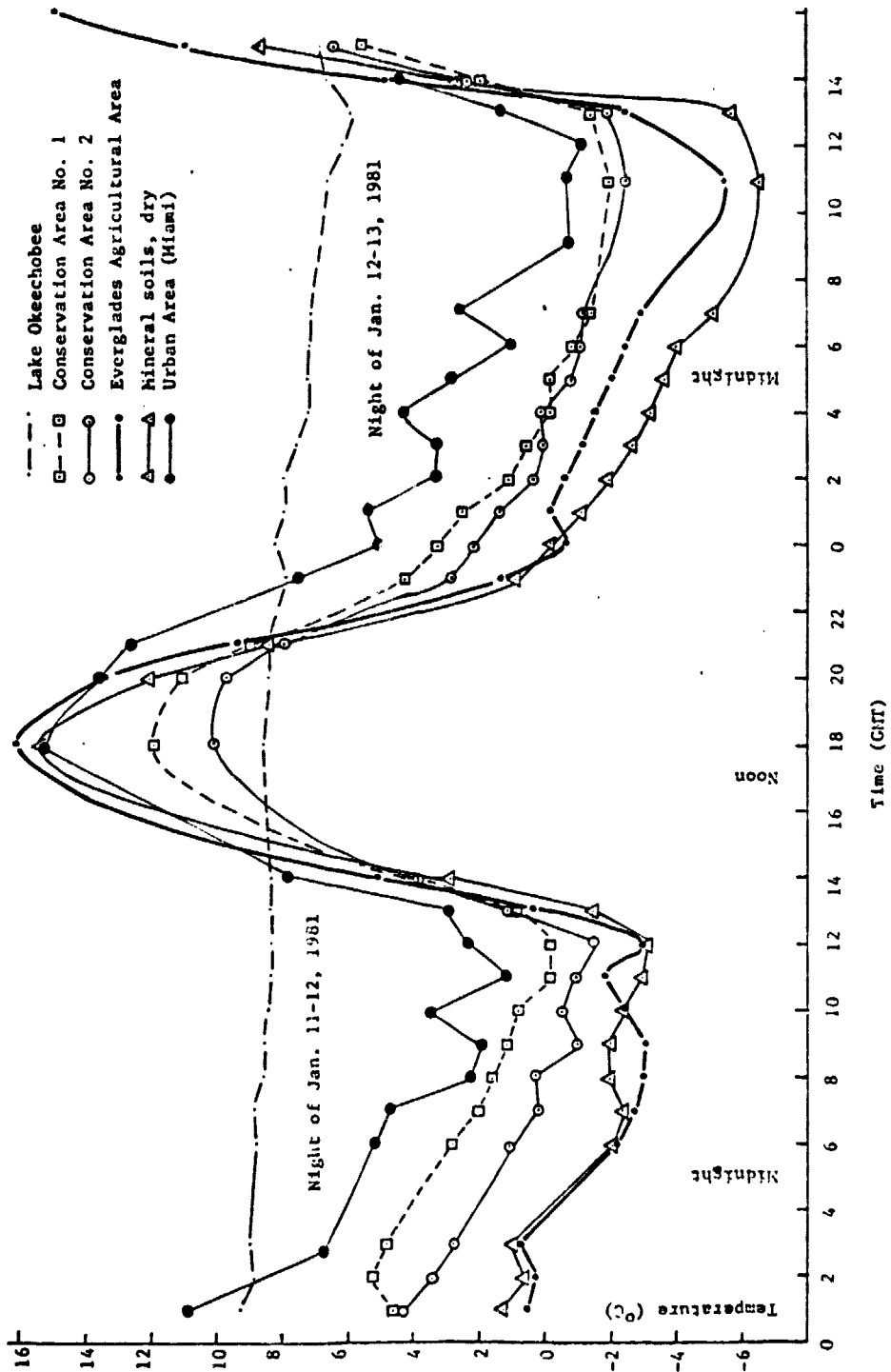
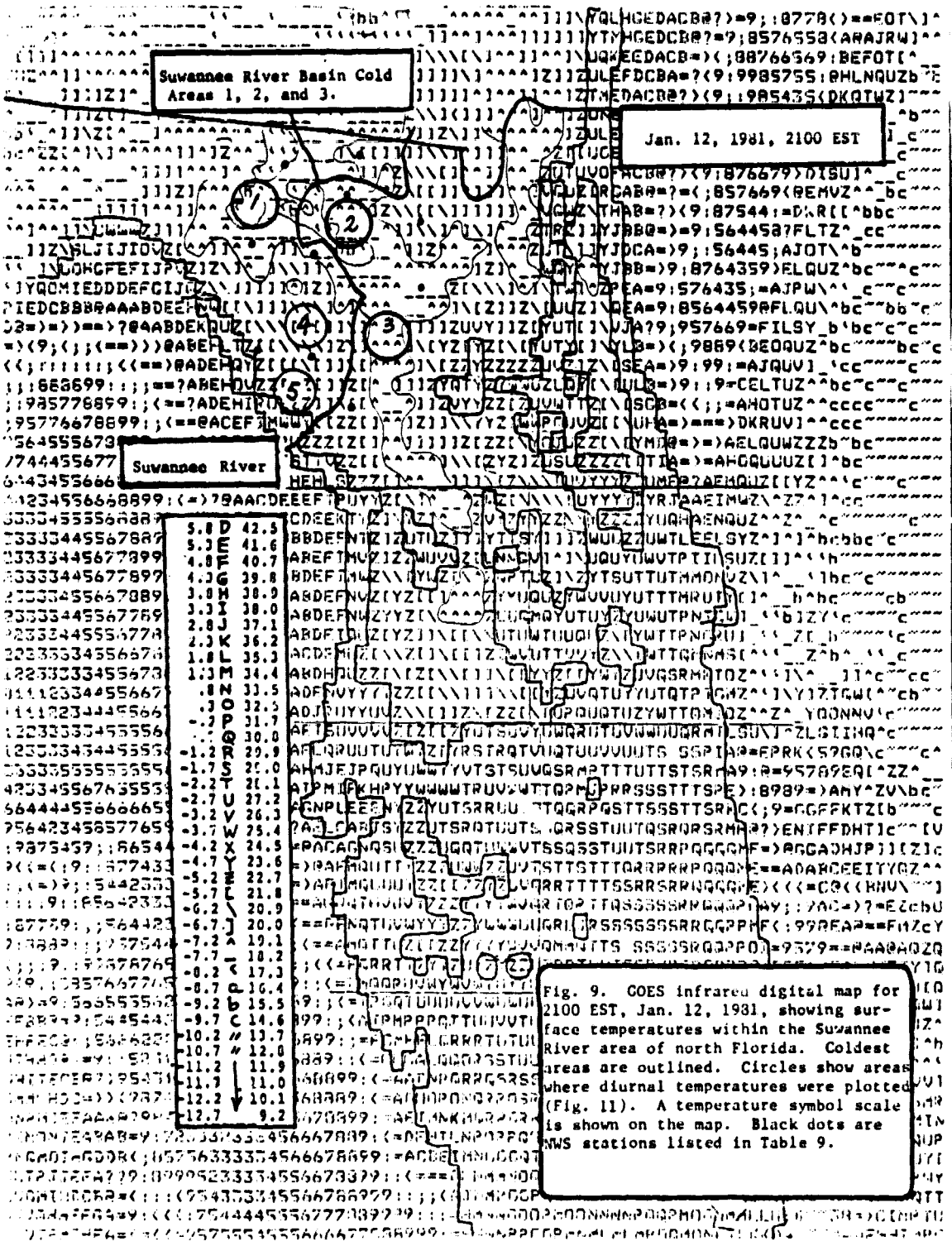


Fig. 8. Diurnal surface temperatures obtained from COES infrared digital data for nights of Jan. 11-12 and 12-13, 1981, during a severe freeze period in Florida.



Suwannee River Basin Cold Area 1, 2, and 3.

Jan. 12, 1981, 2100 EST

Suwannee River

5.0	D	42.5
5.3	E	41.6
4.8	F	40.7
4.3	G	39.8
3.8	H	38.9
3.3	I	38.0
2.8	J	37.1
2.3	K	36.2
1.8	L	35.3
1.3	M	34.4
.8	N	33.5
.3	O	32.6
-.2	P	31.7
-.7	R	30.8
-1.2	S	29.9
-1.7	T	29.0
-2.2	U	28.1
-2.7	V	27.2
-3.2	W	26.3
-3.7	X	25.4
-4.2	Y	24.5
-4.7	Z	23.6
-5.2	A	22.7
-5.7	B	21.8
-6.2	C	20.9
-6.7	D	20.0
-7.2	E	19.1
-7.7	F	18.2
-8.2	G	17.3
-8.7	H	16.4
-9.2	I	15.5
-9.7	J	14.6
-10.2	K	13.7
-10.7	L	12.8
-11.2	M	11.9
-11.7	N	11.0
-12.2	O	10.1
-12.7	P	9.2

Fig. 9. GOES infrared digital map for 2100 EST, Jan. 12, 1981, showing surface temperatures within the Suwannee River area of north Florida. Coldest areas are outlined. Circles show areas where diurnal temperatures were plotted (Fig. 11). A temperature symbol scale is shown on the map. Black dots are AWS stations listed in Table 9.

Fig. 10. HCMM derived apparent thermal inertia image from nighttime Dec. 15 and daytime Dec. 17, 1978, data. Areas in north Florida in the Suwannee River Basin were clear although overall sky conditions were poor southward. The thermal inertia patterns of the Suwannee River Basin agreed with diurnal GOES thermal data.

PRECEDING PAGE BLANK NOT FILMED

same general pattern as GOES and LANDSAT false color imagery. Therefore, we decided to examine the thermal properties of the area and to obtain thermal inertias for the region in preparation for construction of a thermal inertia map for Florida. GOES surface temperatures from January 12-13, 1981 (Fig. 11), were used to obtain cyclic diurnal surface temperature curves for five areas in the Suwannee River Watershed. As an accuracy check for GOES temperature, maximum and minimum temperatures from NOAA cooperative observer stations in the Suwannee River Basin were tabulated in Table 9 (approximate location of each site indicated by black dots but not individually identified on Fig. 9). The five areas, shown in Fig. 9, are regions which appeared colder than surrounding areas early in the evening (1900 to 2100 EST). Of the five areas, Area 2 appeared generally the earliest and also the coldest. The diurnal surface temperatures are shown in Fig. 11. Area 2 has a larger diurnal amplitude than other Areas, which indicates different thermal inertia and thermal properties. Areas 1, 2, and 3 are found in higher well-drained elevations (100 to 150 ft) whereas areas that are warmer at night (4, 5) are found in lower, poorly-drained elevations (less than 100 ft).

A strip of mineral soil is found along the southeast coast of Florida. This mineral soil has been highly drained. It is highly urbanized, with agricultural development at the south and north ends. This strip is thermally very distinct from the wetter Everglades to the west (Figs. 2 and 3). The diurnal GOES surface temperatures for the Miami urban area are shown in Figs. 7 and 8. This area shows an urban heat island effect because the midday temperatures are high, but the nighttime temperatures do not drop as low as the Everglades Agricultural Area. Fig. 8 also shows the distribution of diurnal surface temperatures for Lake Okeechobee and for a mineral soil area west of Lake Okeechobee.

4.4. Thermal inertia analysis and interpretation

4.4.1. Thermal inertia classification using the GE Image-100 system

The HCMM apparent thermal inertia map (Fig. 5) of February 1-3, 1979 (AAO-281-06580-5, HCMM14, File 5) was digitized using the GE Image 100 and PDP 1145 Mini-Computer System. Results showed that the state can best be divided into 5 thermal inertia classes. Each class contained 5 grey scales (grey scales range from 0 to 255), beginning with grey scale 40 (Table 10) and ending at grey scale 80. This range (40-80) of grey scales covered the entire state except for water areas (Table 10). On comparison with a general soil map of the state (Fig. 12), an apparent thermal inertia image from HCMM data (Fig. 5), and a low-temperature map generated from GOES (such as Fig. 9), the following thermal inertia classes (Table 11) are formed, based on information from HCMM scene AAO-281-06580-5 digital data processed using the Image 100 system. Thermal inertia class 2 corresponds well with coldest areas detected by GOES in the Central Florida Ridge and in the drained Everglades Agricultural Area, which we have monitored since 1977 (Chen *et al.*, 1979). Thermal inertia class 1 included small cold pockets scattered within class 2. These small cold areas are known to be present from reports from citrus growers and Cooperative Extension Service personnel. These details are not resolved by the low resolution (8-km) GOES images, but appeared in

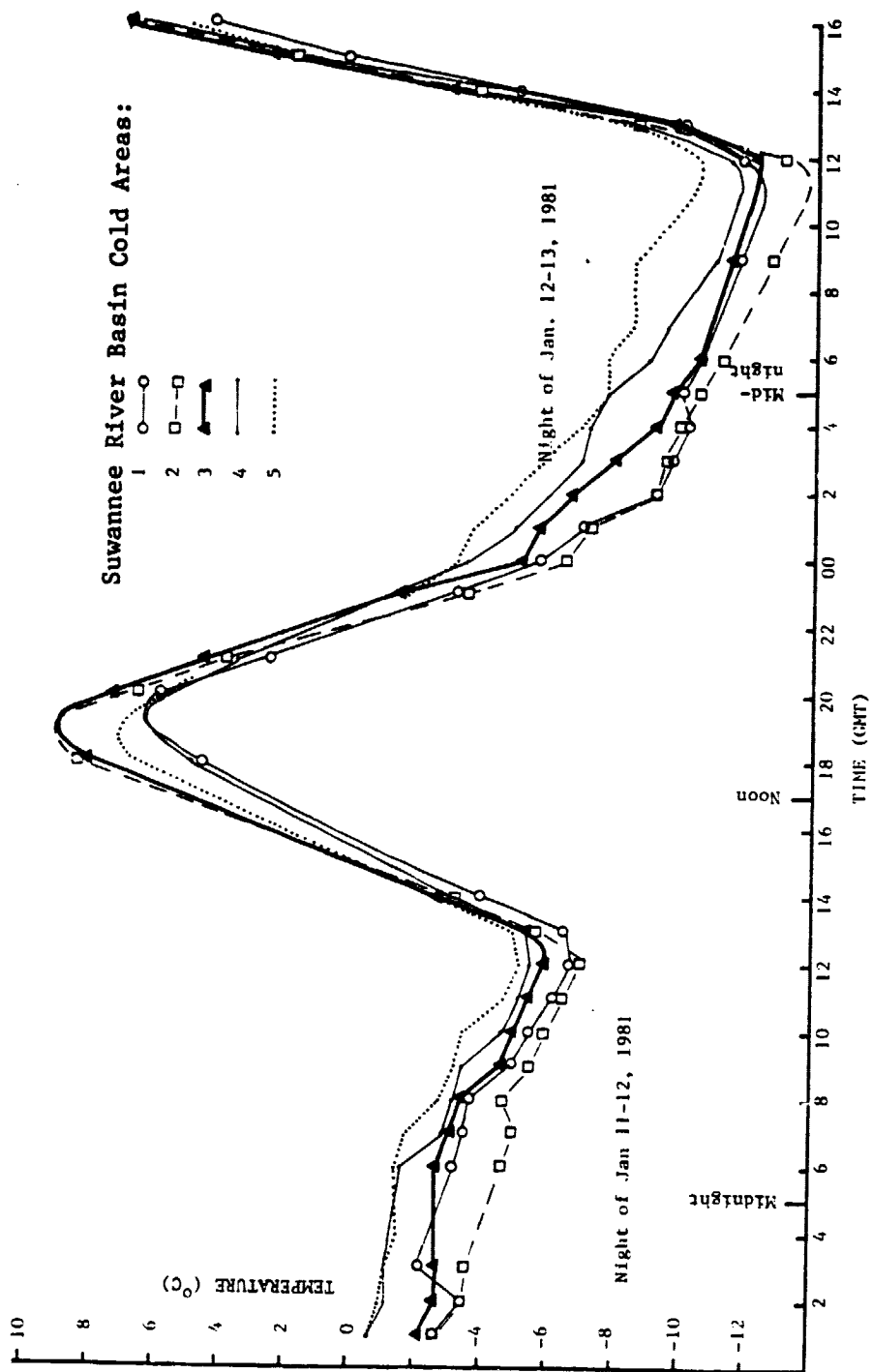


Fig. 11. GOES diurnal surface temperatures for 5 areas in the Suwannee River Basin area (see Fig. 9).

Table 9. Maximum and minimum temperatures from January 12-13, 1981, for NOAA cooperative observer stations in the Suwannee River basin of North Florida. Approximate location of the cities are indicated in Fig. 9 (black dots). Source: Climatological Data, Florida, 85, No. 1, National Climatic Center, Asheville, NC, 1981.

Station	Temperature (°C)	
	Max.	Min.
Cross City 2 WNW	5.6	-12.2
High Springs	10.0	- 7.8
Jasper	5.0	-11.7
Lake City 2 E	4.4	-10.6
Live Oak	10.0	-12.2
Madison 4 N	8.9	-10.0
Mayo	4.4	-11.1
Perry	8.3	-11.7
Steinhatchee 6 ENE	7.2	-11.1
Usher Tower	10.0	-11.7
Average	7.4	-11.0

Table 10. Thermal Inertia Classes for Florida from Feb. 1-3, 1979 Day-Night HCMM Data.

*** 1-CHANNEL LEVEL SLICER ***

WARNING: WIPES OUT THEME TRACKS

TYPE CHANNEL AND #-OF-SLICES, OR E(X)IT 1 8

EQUAL SLICES? (Y/N)
N

INPUT 8 LOWER LIMITS AND FINAL UPPER LIMIT
40 45 50 55 60 65 70 75 80

THEME(1): 40 TO 44
THEME(2): 45 TO 49
THEME(3): 50 TO 54
THEME(4): 55 TO 59
THEME(5): 60 TO 64
THEME(6): 65 TO 69
THEME(7): 70 TO 74
THEME(8): 75 TO 80
E(X)IT OR (R)ECYCLE ?

ORIGINAL PAGE 19
OF POOR QUALITY

*** AREA SUMMARY (DS/1.0) ***

	I	MEMORY		I	LANDSAT		I	
	I	PIXELS	PERCENT	I	PIXELS	ACRES	HECTARES	I
	I			I				I
TRAIN	I			I				I
AREA	I	0.	0.0%	I	0.	0.0	0.0	I
	I			I				I
ALARM	I	0.	0.0%	I	0.	0.0	0.0	I
	I			I				I
THEME 1	I	2600.	1.0%	I	2610.	2918.1	1181.0	I
	I			I				I
THEME 2	I	1207.	0.5%	I	1212.	1354.7	548.2	I
	I			I				I
THEME 3	I	15476.	5.9%	I	15537.	17369.7	7029.5	I
	I			I				I
THEME 4	I	71647.	27.3%	I	71927.	80414.1	32543.6	I
	I			I				I
THEME 5	I	23208.	8.9%	I	23299.	26047.8	10541.6	I
	I			I				I
THEME 6	I	5962.	2.3%	I	5985.	6691.5	2708.1	I
	I			I				I
THEME 7	I	4038.	1.5%	I	4054.	4532.1	1834.1	I
	I			I				I
THEME 8	I	4295.	1.6%	I	4312.	4820.6	1950.9	I

Table 11. Thermal inertia classes for Florida based on HCMM image AAO-28106580-5 and using the Image-100 Image Analyzing System to determine areas with equal thermal inertia as defined by grey scales. Data digitized: HCMM A-A0281-06580-5 (HCMM14, File 5). Data formatted from Feb. 1 (night) and Feb. 3 (day), 1979, IR temperatures.

% Area	Thermal Inertia Class	Thermal Inertia Area
1.04%	1 (Theme 2)	Lowest thermal inertia class. Numerous small areas scattered within drained organic soils of the Everglades Agricultural Area and in the deep, sandy, well-drained soils of the Central Florida Ridge Land Resource Area. ^{1/}
12.3%	2 (Theme 3)	Drained organic soils of the Everglades Agricultural Area and deep, sandy, well-drained soils of the Central Florida Ridge Land Resource Area.
56.9%	3 (Theme 4)	Peninsular Florida Flatwoods Land Resource Area, except areas covered by Themes 5,6,7,8.
18.5%	4 (Theme 5)	Coastal Zones and Wetlands: 1. Between Waccasassa Bay and Tampa Bay along west coast of central Florida 2. St. Augustine and Kennedy Space Center along east coast of central Florida 3. Tsala Apopka Lake region 4. Green Swamp
4.8%	5 (Themes 6, 7, and 8)	Shoreline, river, Water Conservation Area #1.
3.1%		Shoreline, Water Conservation Area #1, part of natural Everglades.
3.3%		Water Conservation Area #2, natural Everglades.

^{1/} Generally too small to be resolved by GOES

the high resolution (600-m) HCMM images. The thermal inertia classes agree well with information obtained from GOES images (Chen and Martsof, 1982). The area north of Lake Okeechobee appeared quite cold (GOES images) during the 1980-81 and 1981-82 winters, but did not appear to be relatively as cold based on apparent thermal inertia image (Fig. 5). This area generally has flat topography and high water table, poorly drained soils of the South Florida Flatwoods Land Resource Area, which usually will have a higher thermal inertia, and therefore will not usually appear cold. However, if drought conditions exist, as in 1980-82, the area can become cold. During the winter of 1978-79, climatological data (National Oceanic and Atmospheric Administration, 1979) showed higher than average rainfall amounts (Table 12), whereas several subsequent years showed lower than average rainfall amounts.

4.4.2. Correlation of HCMM apparent thermal inertia with HCMM surface infrared temperatures

A computer program was developed to read the HCMM CCT's, average the values in a 5-pixel x 5-pixel array, and print a symbol map of these averaged pixels. The IR pixels of such a symbol map represent 20 to 25% of the area of a GOES IR pixel. This process reduced the symbol map data to a manageable size for displaying the Florida peninsula. Reduced symbol maps for both nighttime IR temperature data of February 3, 1979, and apparent thermal inertia based on February 1 and 3 day-night overflights were developed (Figs. 13A and 13B). Data were extracted from a west-to-east cross-section of north central Florida (Figs. 12 and 13A, 13B, labeled A...A'), and the values tabulated (Table 13). This cross-section passes through persistent cold areas as indicated by GOES and therefore includes some of the lowest temperatures in the state during this period. Values in Table 13 are plotted in Fig. 14. Symbols that indicated surface waters were not included in Fig. 14 because thermal inertia of surface water areas were found to be nonlinearly related to temperature, causing errors in linear regression analysis of grey scale versus temperatures. Regression statistics of apparent thermal inertia (y) and night-IR (x) (Table 13) are:

Number of points (n) = 69
Mean temperature (\bar{x}) = -2.9°C
Mean apparent thermal inertia (\bar{y}) = 56.8

Standard deviation (Sx) = $+1.36^{\circ}\text{C}$
Standard deviation (Sy) = $\bar{11.95}$

Linear regression equation: $y = 7.07x + 77.5$
Correlation coefficient (r): 0.81

Comparing Table 11 and Fig. 14, thermal inertia classes derived from February 1 and 3, 1979, nighttime and daytime data, respectively, can be associated with the following nocturnal temperatures of February

Table 12. Rainfall and departures from the means from 1979 and for 1980 that determine antecedent surface moisture conditions for periods immediately before the January-February winter period of 1980 and 1981, respectively. Source: Climatological Data, Florida, Annual Summary, National Climatic Center, Asheville, NC, 83, No. 13, 1979, and 84, No. 13, 1980.

Climatic Zone	1979 Rainfall (inches)			1980 Rainfall (inches)		
	Annual (Jan.-Dec.) ppt. ^{1/}	dep. ^{2/}	(July-Dec.) ppt. dep.	Annual (Jan.-Dec.) ppt. dep.	(July-Dec.) ppt. dep.	
Northwest (18) ^{3/}	72.32	12.47	38.54 10.49	59.99 0.14	24.73 -7.23	
North (22)	61.21	6.39	32.51 1.33	51.25 -3.57	23.75 -7.23	
North Central (17)	60.72	7.05	34.52 3.18	46.49 -7.19	25.12 -5.24	
South Central (29)	59.03	5.85	33.60 2.51	43.90 -9.28	23.70 -7.39	
Everglades and Southwest Coast (14)	54.00	0.68	34.18 3.03	45.58 -7.74	26.72 -4.43	
Lower East Coast (12)	60.32	0.79	35.15 1.22	57.97 -1.56	33.69 -1.47	

^{1/} ppt. = total rainfall for the zone.

^{2/} dep. = departure from long-term means based on periods varying from 10 to 29 years.

^{3/} Number of reporting stations in each zone.

Fig. 13. Five by five blanks of HCNV sheets averaged from Night IR data of Feb. 3, 1979 (A) and from Apparent thermal Inertia data based on Feb. 1-3 1979 day-night overflights (B), for use in relating apparent thermal inertia with nighttime surface temperatures. A...A' identifies the row of pixels listed in Table 13. See also Fig. 12.

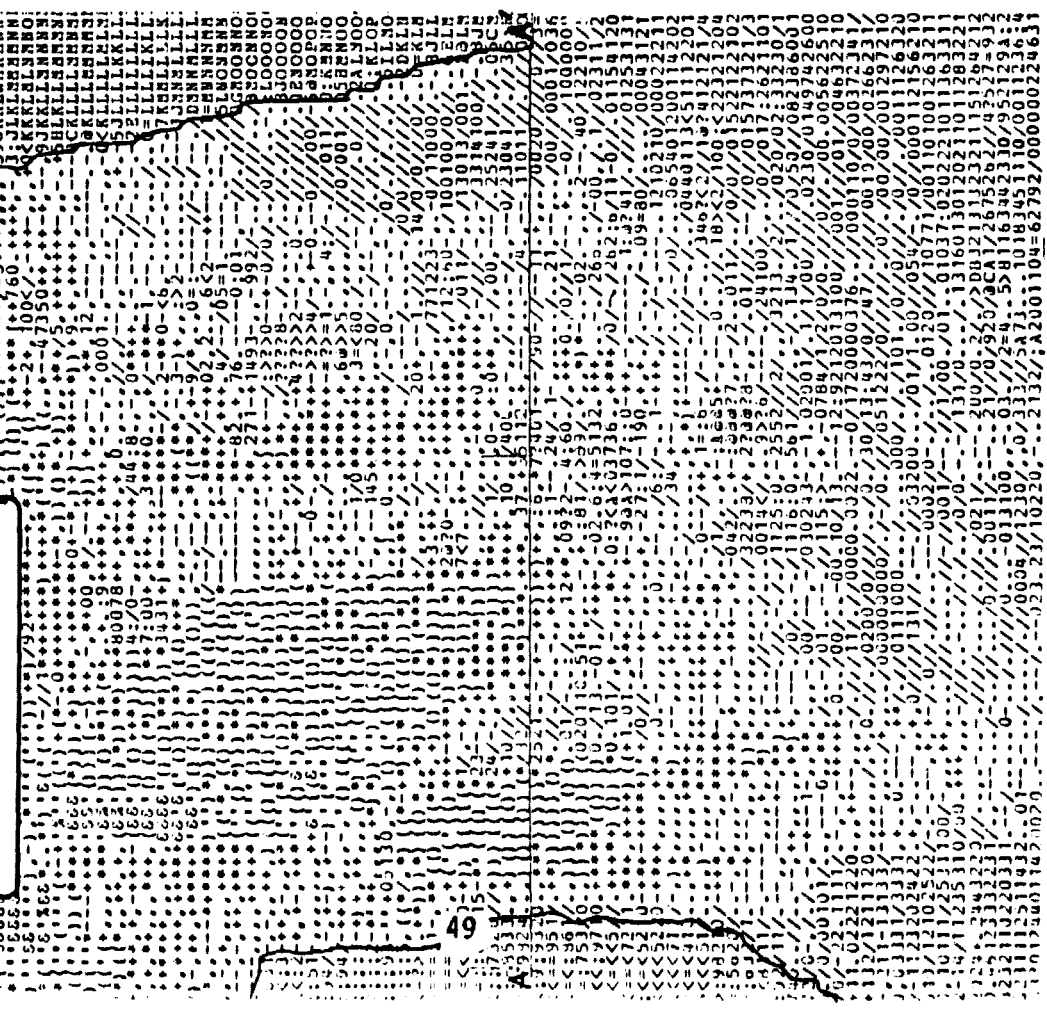
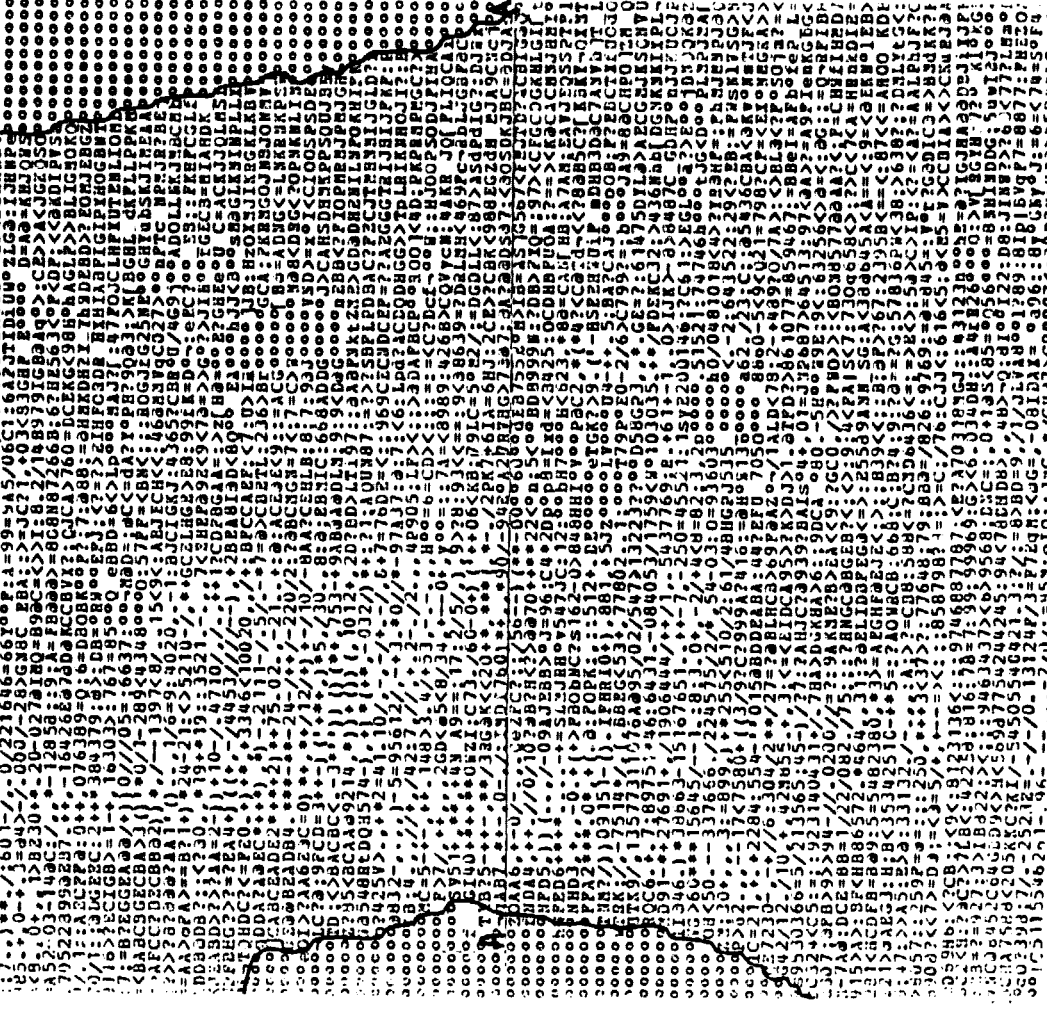


Fig. 14. AAO-281065805 Thermal Inertia, North Central FL. The grid shows thermal inertia values for various pixels, with a large 'A' in the top left corner. The values are arranged in a grid format, with some cells containing numerical values and others being blank.



ORIGINAL PAGE IS OF POOR QUALITY

ORIGINAL PAGE IS OF POOR QUALITY

Table 13. HCMM thermal inertia and night-IR temperatures for day-night pair of Feb. 1-3, 1979. Data pair was taken from a cross-section in North Central Florida (Fig. 13-A and 13-B, A...A'). Temperatures are uncorrected.

Thermal Inertia (Grey Scales)	Night-IR (°C)	Thermal Inertia (cont.)	Night-IR (cont.)
62	-2.7	79	0.10
63	-2.7	83	-1.5
52	-3.5	69	-1.5
43	-4.8	68	-1.1
39	-5.2	59	-2.7
40	-4.8	52	-3.9
42	-4.8	61	-3.5
41	-5.2	61	-3.1
45	-4.8	52	-3.1
42	-4.8	55	-3.1
41	-5.2	61	-3.5
44	-4.4	62	-2.7
55	-2.3	60	-2.7
70	-0.7	61	-3.1
74	-1.1	61	-3.1
65	-2.3	65	-2.3
70	-2.3	80	-0.33
52	-3.5	61	-2.7
51	-3.5	52	-3.5
45	-3.9	56	-3.1
38	-4.2	57	-3.1
39	-4.2	61	-2.7
40	-4.8	76	-1.5
41	-4.2	80	-1.5
41	-4.2	65	-1.9
39	-4.2	72	-1.5
54	-2.7	71	-1.5
45	-3.9	63	-2.3
44	-3.9	64	-2.3
42	-4.4	58	-2.7
54	-3.5	61	-2.3
49	-0.7	65	-2.3
66	0.9	71	-2.3
62	-3.9	62	-1.9
47	-0.7		

ORIGINAL PAGE IS
OF POOR QUALITY

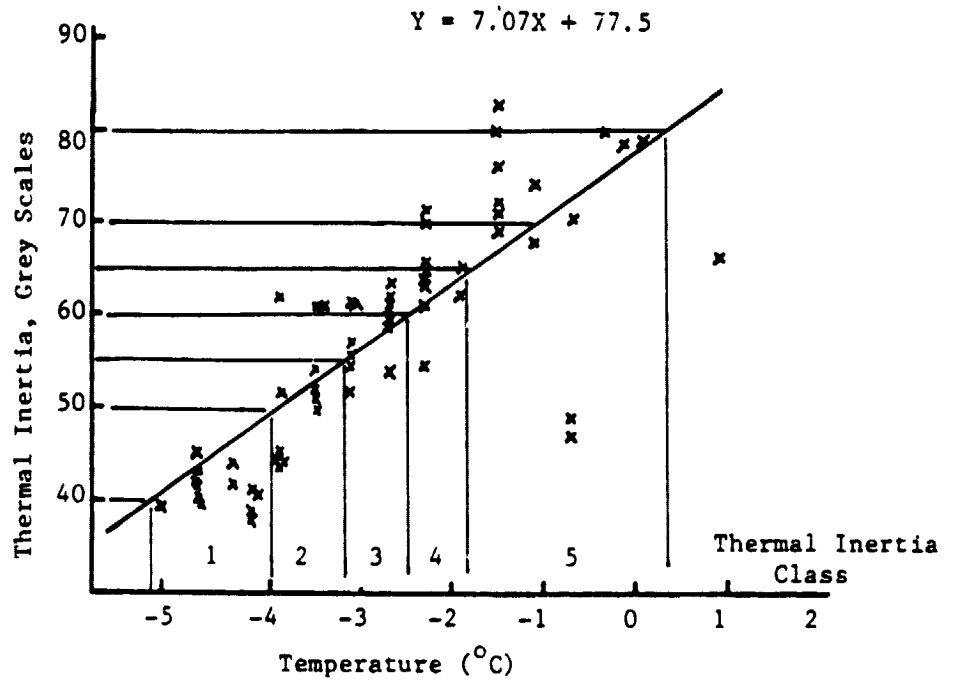


Fig. 14. Linear regression of thermal inertia (grey scales) and temperatures for the cross section AA' (Fig. 13).

1, 1979. It can be seen that in this case, the thermal inertia classes are separated by temperatures of approximately 1°C:

Thermal inertia class 5	5.5 to 3.5°C
Thermal inertia class 4	3.5 to 2.8°C
Thermal inertia class 3	2.8 to 2.0°C
Thermal inertia class 2	2.0 to 1.4°C
Thermal inertia class 1	colder than 1.4°C

Temperatures given above have been adjusted by adding 5.5°C to correct for the HCMM calibration (HCMM Users' Guide, 1980).

4.4.3. Fourier analysis of GOES temperatures

Diurnal temperatures from GOES for two data sets (February 26-27, 1980, and January 11-13, 1981), one each from wet (1979-80) and dry (1980-81) winter seasons illustrate diurnal amplitudes which resulted from differences in relative surface water content of the areas resulting from long-term wet or dry antecedent conditions (Figs. 7 and 8). Table 12 shows amounts of rainfall for periods immediately before February, 1980, and January, 1981. The entire state showed higher than average rainfall for 1979 and lower than average rainfall for 1980, especially for the latter half of the year (July-Dec. columns). Diurnal temperature amplitudes of the drained Everglades Agricultural Area were larger than those of the three Water Conservation Areas, which indicates that the former has a smaller thermal inertia than the latter. Water Conservation Area #1 showed a larger diurnal amplitude than Water Conservation Area #2 for wet antecedent conditions (Fig. 7), whereas the difference between the diurnal amplitudes was less for dry antecedent conditions (Fig. 8). Average diurnal amplitudes for the Water Conservation Areas were larger for data from January 12-13, 1981 (dry) than for data from February 26-27, 1980 (wet). Diurnal amplitudes from GOES could be used to estimate thermal inertia to compare with HCMM apparent thermal inertia.

An equation representing diurnal surface temperatures can be written in a Fourier series as follows:

$$\theta(0,t) = \theta_a + \sum_{k=1}^{\infty} (A_k \cos k\omega t + B_k \sin k\omega t) \quad [1]$$

where θ is the temperature in °C, t is the time in sec, θ_a is the average temperature at the surface, k is the number of harmonics, A_k and B_k are the Fourier coefficients, and ω is the diurnal frequency ($=k \cdot 2\pi/86400 \text{ sec}^{-1}$). Surface temperatures from GOES were used to obtain the coefficients and the equation which describes the diurnal temperature wave. One result is shown in Fig. 15 for Everglades Agricultural Area hourly data from GOES over the interval 0600 GMT (0100 EST), January 12, 1981, to 0600 GMT (0100 EST), January 13, 1981. The equation (with coefficients) is:

$$\begin{aligned} \theta(0,t) = & 3.7 - 8.33 \cos(\omega t) - 0.7 \sin(\omega t) + 3.91 \cos(2\omega t) - \\ & 0.51 \sin(2\omega t) - 0.92 \cos(3\omega t) + 0.12 \sin(3\omega t) - \\ & 0.45 \cos(4\omega t) + 0.09 \sin(4\omega t) \end{aligned} \quad [2]$$

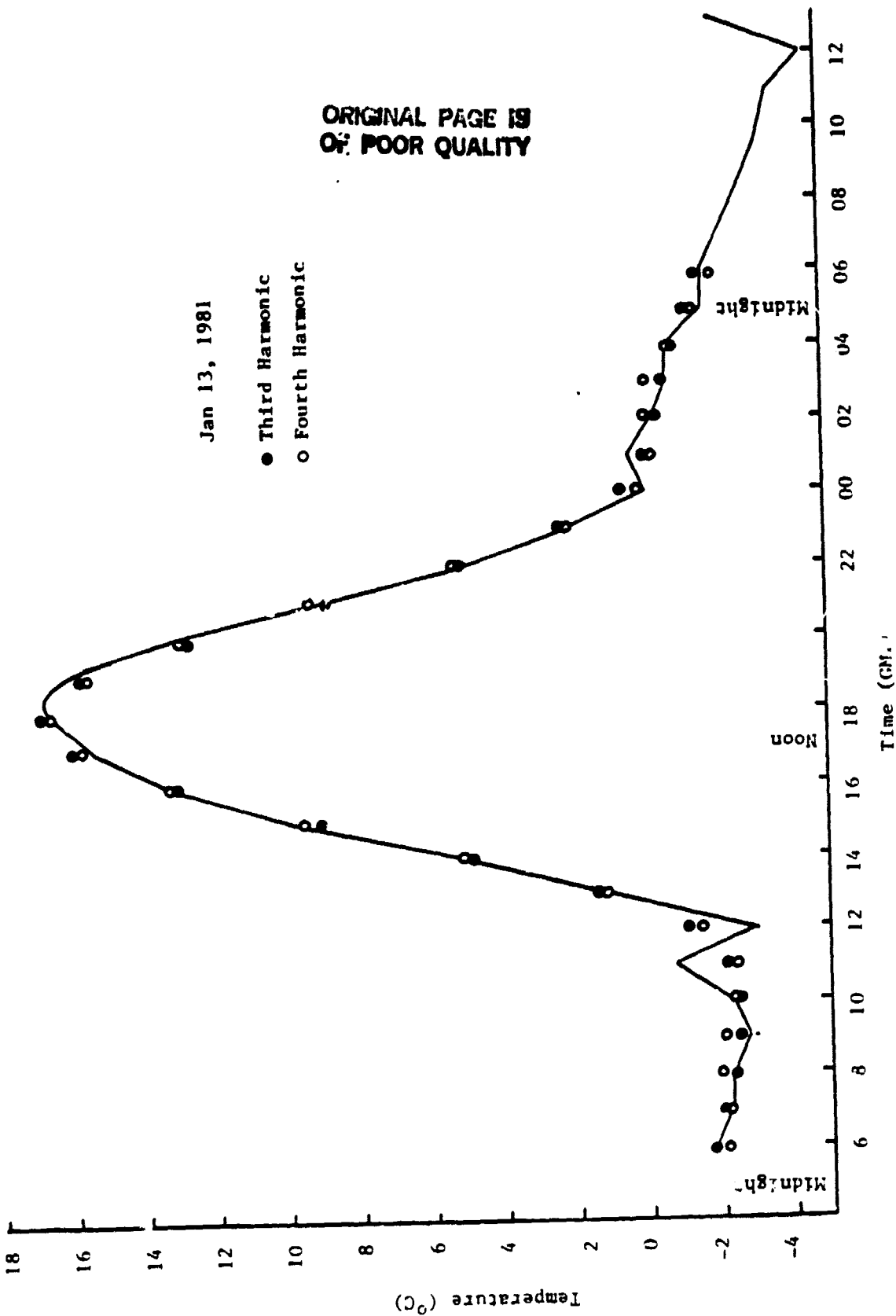


Fig. 15. Fourier fit of GOFS diurnal temperatures in the Everglades Agricultural Area for data from Jan. 12-13, 1981.

The result could be used to estimate thermal inertia independent of HCMM apparent thermal inertia both as a check and also to be used to fill the HCMM diurnal surface temperature data gap, assuming the majority of the contribution can be extracted from the first harmonic.

4.4.4. Prediction of moisture availability and thermal inertia from Carlson's model

HCMM data were used in conjunction with Carlson's model (Carlson and Boland, 1978; Carlson et al., 1981) to predict thermal inertia and moisture availability of the surface. Carlson's model was selected because it is a thorough energy balance model and because it was applied earlier to HCMM data.

HCMM data from the day-night sequence of February 3 (day) and February 1 (night), 1979, were selected to apply to the model. This day-night sequence was selected because of good sky conditions and because nocturnal GOES images for February 1, 1979, were available. The model was applied to a wet and a dry area in north central Florida (Fig. 16). They are:

- (1) Waccasassa Flats (wet, area 1, 2, and 3).
- (2) Newberry Sandhills (dry, area 4 and 5)

The HCMM (HCMM13) data and products used are:

- (1) February 1, 1979, Night-IR
- (2) Apparent thermal inertia, from February 3 and February 1 day-night pair
- (3) Temperature difference, from February 3 and February 1 day-night pair

Parameters that we specified using in the model were:

- (1) Lat (Latitude): 29.5°N
- (2) Long (Longitude): 82.5°W
- (3) Emissivity of the surface: 1.0
- (4) Albedo: 0.32, the high value is used to account for brighter wintertime surfaces and for the presence of some clouds; the high albedo has the effect of decreasing solar radiation reaching the ground
- (5) Z_0 , roughness length: 100 cm (forest--longleaf pines and turkey oaks)
- (6) BTemp, 2.95-m depth ground temperature, constant: 289°K
- (7) Initial shelter-height temperature (at 0600 local time): 271.5°K, determined from an average of NCC data for the region

HCMM-4
NORTH
FILE # 2
CORRECTED

Fig. 16. HCMM (AAO-281-065804) temperature difference data from Feb. 1-3, 1979. This set of data is used to obtain a day temperature (6°C was added to the temperature to correct HCMM data) to use with Carlson's model. Areas used are labeled 1, 2, and 3 (wet) and 4 and 5 (dry). The areas are also located by x's in Fig. 12.

- (8) Temperature, dewpoint temperature, wind speed, and wind direction with height based on radiosonde data from Ruskin, Florida, at 1200Z (0700 EST), February 1, 1979
- (9) Precipitable water estimated from RADCOM (Weinreb and Hill, 1980): 0.5 cm
- (10) Surface temperature gradients and surface pressure gradients, estimated from weather maps
- (11) K_M , the turbulent diffusivity: $500 \text{ cm}^2/\text{sec}$ for flow through and over a forest canopy surface, which has roughness elements that protrude into the surface boundary layer.
- (12) Several other parameters, such as a table of solar transmission coefficients as a function of wavelength, HCMM satellite overpass times, frequency of printed output summary, month, day, ground depth parameters, and other program control parameters, such as starting time (usually 0600 local time), ending time, and time zone with respect to Greenwich mean Time

The Carlson model uses satellite day-night overpass data in three basic steps (Carlson et al., 1981):

- (1) Model is run for about 24-hour time conditions, with a range of fixed moisture availability (MA) and thermal inertia (TI) values that predict daytime surface temperatures and nighttime surface temperatures at the time of satellite overpass. Clear sky conditions are assumed, and the energy balance is computed at 4-minute time steps during the day and 2-minute time steps at night.
- (2) Multiple regression equations are then used to develop predictor equations for MA and TI based on the daytime surface temperatures and nighttime surface temperatures.
- (3) Registered satellite day and night pixel values of surface temperature are then used to predict MA and TI by pixels or by clusters of pixels.

The Carlson model can print out the energy budget at any time as specified. Final outputs can also include total daytime net radiation, total nighttime net radiation, daytime latent heat exchange, nighttime latent heat exchange, the Bowen ratio, total evapotranspiration, daytime sensible heat exchange, nighttime sensible heat exchange, daytime ground temperature (at the 10-cm depth at the satellite overpass time) and nighttime ground temperature (at the 10-cm depth at the satellite overpass time).

Parameters that were specified for the model were listed earlier. However, because of our inexperience in Florida with the model, we had to make a number of computer runs to develop day-night pairs of model-predicted surface temperatures that were within the range of observed HCMM values. Finally, because HCMM values were estimated from February 3, 1979, daytime values and February 1, 1979, nighttime values, the tem-

perature differences had to be readjusted also. Sequential runs led us to make the following adjustments in input parameters to be more realistic.

- (1) Shelter height temperature throughout the north and north-central climate region was used for the 1000 mb temperature rather than the Ruskin radiosonde data at the surface.
- (2) Albedo was raised from 0.24 to 0.32 in order to bring model-predicted daytime temperature in range with the HCMM daytime temperature.
- (3) Turbulent diffusivity for both heat and water vapor transfer was increased to be more realistic with forest and rough surfaces that protrude into the free air stream.
- (4) Ground temperature at 2.95 m was decreased from an estimated 292°K to an estimated 289°K, which improved model predictions.

The day-night temperature pairs for input into the model to predict thermal inertia and moisture availability are shown in Table 14.

Since a February 3 (day) reading was not available on our CCT's, we used the February 1 (night) plus the temperature difference (February 3 to February 1) to find a February 3 day-IR image. The NASA-Goddard temperature difference pixels overlaid exactly the February 1 (night) IR temperature pixels. Since they were elongated HCMM data sets that included more than one primary scene, they covered most of the state. Climatic data (National Oceanic and Atmospheric Administration, 1979) were examined to obtain the climatic mean daily maximum and minimum temperatures of the north and north central Florida climate zones over the period of January 28 to February 3, 1979. We found the day-night pair of February 1 to be 55°F and 29°F, but the day-night pair for February 3 was 61°F and 34°F. Therefore, we reduced the February 3 day-IR data by 6°F (3.3°C). 5°C was added to all of the IR data to correct for HCMM calibration offset (HCMM User's Manual, 1980).

The vertical moisture profile was estimated from the nearest radiosonde sounding, taken at Ruskin, Florida, at 1200 GMT (0700 EST). The sounding from Ruskin is near Tampa Bay and represents the best compromise for an average sounding along the length of the peninsula. However, there may be some local effects of Tampa Bay or the Gulf of Mexico near the earth's surface. Moisture, temperature and pressure from soundings were inputted into the RADCOM model (Weinreb and Hill, 1980) to compute effect of moisture and gases on surface temperature. Based on RADCOM model calculation, HCMM-derived surface temperatures were increased by 1°C to account for atmospheric absorption.

Predicted thermal inertia (TI) and moisture availability (MA) predicted from model calculations for areas 1, 2, 3, 4, and 5 are shown in Table 15.

Carlson (personal communication) showed that MA is equivalent to $R_a / (R_a + R_s)$, where R_a is a surface (e.g., canopy) aerodynamic resis-

Table 14. Day-night temperature pairs for input into Carlson's model to predict thermal inertia and moisture availability.

	Area	Temperature	
		Feb. 3 (day)	Feb. 1 (night)
1	Waccasassa Flats (wet)	285.0°K	275.3°K
2	"	284.5	274.9
3	"	285.1	274.5
4	Newberry Sandhills (dry)	287.0	272.4
5	"	288.2	272.8

Table 15. Predicted thermal inertia (TI) and moisture availability (MA) for areas 1, 2, 3, 4 and 5.

Area	Predicted TI cal/cm ² /sec ^{1/2} °K	Predicted MA Dimensionless
1 Waccasassa Flats (wet)	0.0886	0.717
2 "	0.0866	0.965
3 "	0.0796	0.771
4 Newberry Sandhills (dry)	0.0539	0.379
5 "	0.0550	0.046

tance and R_s is a surface internal resistance (e.g., ensemble stomatal resistance for a canopy). However, this generalized form can be applied to any surface whether it is vegetated or not.

Moisture availability (MA) by definition would normally be expected to be between 0.0 and 1.0, i.e., near 0.0 for a nonevaporating surface and near 1.0 for a freely evaporating surface. MA predicted by Carlson's model (Table 15) appeared to be sensitive to several parameters in addition to the combination of day and night satellite temperatures, including the initial shelter-height temperature, the temperature at the bottom of the substrate (2.95 m), the albedo, and the turbulent diffusivity. The substrate temperature was an average value obtained from data taken during freeze nights in 1978 from stations in Central Florida and is similar to other observations (DuCharme, 1971). We experimented with substrate temperatures of $289 \pm 3^\circ\text{K}$. We found that at the higher temperature (292°K), the predicted MA for the 5 temperature pairs in Table 15 had a range of 1.12, but had values as high as 1.32. At the lower temperature (286°K), the range had decreased to 0.697, but had MA values as low as -0.17. MA was also found to be sensitive to changes in initial surface input temperature (at 0600 local time). According to model outputs, an increase in daytime surface temperature (accompanied by a larger diurnal temperature amplitude) had the expected effect of decreasing MA. A decrease in daytime surface temperature (accompanied by a smaller diurnal temperature amplitude) had the expected effect of increasing MA. The model thus illustrated that if the diurnal temperature amplitudes are too large or too small, its predicted MA will not always fall between 0 and 1.

Thermal inertias (TI) predicted from the 5 temperature pairs (Table 15) seemed to be less sensitive to changes of temperature at the substrate layer or any other of the input parameters. Differences in TI between wet and dry areas were predicted to be on the order of $0.03 \text{ cal cm}^{-2} \text{ sec}^{-1/2} \text{ }^\circ\text{K}^{-1}$ under these conditions.

4.4.5. Comparison of HCMM IR data with GOES IR data

Since cloudy conditions were prevalent over Florida during the winter of 1978-79, many frames of HCMM data were of limited use. To partly compensate for lack of usable HCMM data, GOES images were used to provide information to calculate apparent thermal inertia (ATI). A large quantity of GOES winter nighttime infrared data were archived for Florida. By using the Florida data from GOES, we can calculate ATI and provide information to help determine usefulness of the ATI data product. One advantage of using GOES data is that the availability of data each day allowed us to select similar cold events more frequently than with HCMM, and allowed us to calculate ATI over the same surface within a short time period, thereby giving some assurance that thermal inertia of the soil would not have changed significantly during this period.

GOES surface temperatures were compared with calibrated HCMM night-IR data from film transparencies. Also, GOES data one week apart (January 12-13 and 18-19, 1981) were used to calculate ATI using methods in the HCMM User's Guide.

To compare GOES surface temperatures with HCMM surface temperatures, HCMM film transparencies for night-IR data from January 10 and February 1, 1979, were used. Film characteristics were:

January 10, 1979:

Night-IR
Contrast Range: 27-76
Corresponding temperature range: -1.5 to 16.6°C
°C/grey scale: 1.13°C

February 1, 1979:

Night-IR
Contrast Range: 18-75
Corresponding temperature range: -5.2 to 16.2°C
°C/grey scale: 1.34°C

GOES surface temperatures used were from 0400 EST, January 10, and 2300 EST, February 1, 1979. GOES temperatures obtained from the above two images were adjusted to account for time discrepancy between GOES image time and time of passage of HCMM at approximately 0200 EST. A 0.5°C/hour drop in temperature was assumed and is a reasonably conservative value when nights are not excessively cold. Therefore, 1°C was added to GOES temperatures obtained from January 10, 1979, and 1.5°C was subtracted from GOES temperatures obtained from February 1, 1979. Results for temperature estimation for eight areas in south Florida are compared and listed in Table 16. Areas where temperatures were analyzed are shown in Fig. 17.

Average GOES temperatures were 5.9°C and 5.2°C higher than HCMM temperatures, respectively, for the two nights examined (Table 16). Therefore, HCMM data gave temperatures lower than GOES data by approximately 5 to 6°C. Since GOES temperatures compared well with 1.5-m air temperatures (standard error of estimate, +1.6°C; correlation coefficient, 0.86; Chen and Martsolf, 1981), GOES temperatures are probably closer to true values. Perhaps the -5.5°C offset that has been applied to all standard processed HCMM data should be added back to HCMM data, as we did in an earlier section. Results in Table 16 are in agreement with previous HCMM user experience (HCMM User's Guide, 1980).

4.4.6. Calculation of apparent thermal inertia (ATI) using temperatures from GOES satellite data

Equations used to calculate ATI were developed for HCMM data (HCMM Users' Guide, 1980). They are listed below:

$$ATI = NC(1 - a)/\Delta T \quad [3]$$

where $N = 1000$,

C is from Table 11-3, p. 14, HCMM Users' Guide, 1980,

ΔT is obtained from GOES digital IR temperatures,

$a = Kr/(\sin\theta\sin\phi + \cos\theta\cos\phi\cos\delta)$

θ is the latitude on earth,

ϕ is the solar declination, where

Table 16. Comparison of surface IR temperatures derived from HCMM film transparencies with GOES surface IR temperatures for 8 areas in South Florida. Temperature is in °C.

Area Compared	January 10, 1979			February 1, 1979		
	HCMM	GOES ^{1/}	ΔT ^{2/}	HCMM	GOES ^{3/}	ΔT ^{2/}
1. Lake Okeechobee	9.0	13.0 ^{4/}	4.0	6.6	13.0 ^{4/}	6.4
2. Lake Kissimmee				5.6	10.3	4.7
3. Blue Cypress Lake				5.6	8.8	3.2
4. EAA	-1.6	8.5	10.1	-1.2	4.8	6.0
5. Cons. Area #1	6.2	11.0	4.8	4.2	10.0	5.8
6. Cons. Area #2	7.9	11.5	3.6	5.9	10.5	4.6
7. Everglades	5.7	11.5	5.8	3.7	9.5	5.8
8. EAA, West	2.0	9.3	7.3	2.2	7.0	4.8
Average ΔT			5.9			5.2

^{1/} Temperature was estimated by adding 1.0°C to the temperature obtained from the 0400 EST GOES image in order to bring the GOES temperature closer to the time of passage of HCMM (~ 0200 EST).

^{2/} ΔT = GOES temperature - HCMM temperature.

^{3/} Temperature was estimated by adding -1.5°C to the temperature obtained from the 2300 EST GOES image to bring the GOES temperature closer to the passage of HCMM (~ 0200 EST).

^{4/} Water temperatures of Lake Okeechobee, Lake Kissimmee, and Blue Cypress Lake were allowed to stay the same because it has been shown that GOES-detected water temperature of Lake Okeechobee decreases only ~2°C or less throughout a 24-hour period during cold weather events (Chen and Martsoif, 1981).

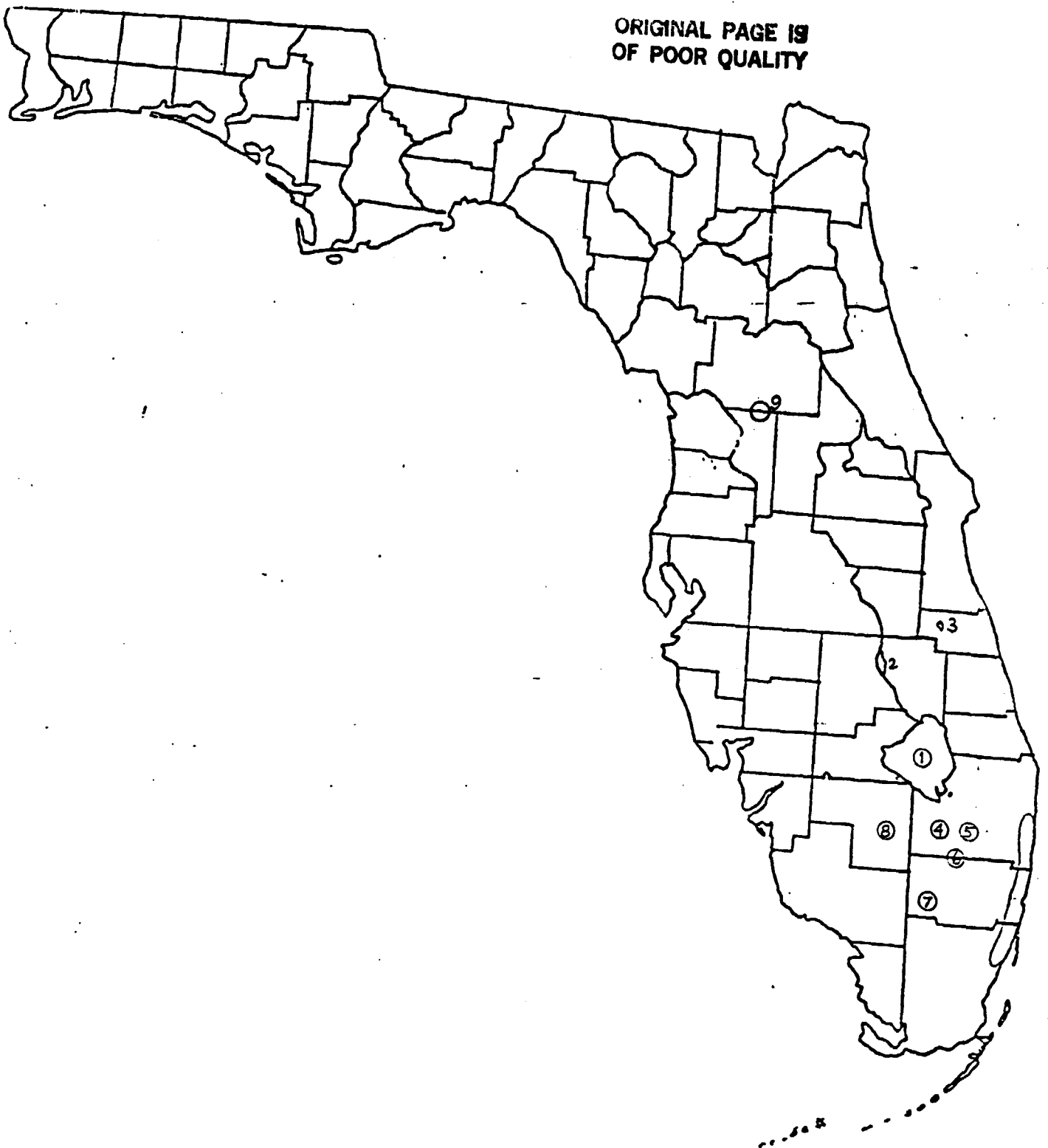


Fig. 17. Map showing the eight areas (1 to 8) where HCMM-derived surface temperatures were compared with GOES surface temperatures. ATI was calculated using ΔT obtained from GOES from Area 4 and Area 9. County lines are shown on the map.

$$\phi = 0.4091 \sin \left(\frac{2\pi(\text{Day} - 80.3)}{365} \right)$$

δ is the hour angle at local noon,

$$K = 1 + 0.0167 \sin \left(\frac{2\pi(\text{Day} - 93.5)}{365} \right)$$

r is reflectivity.

ΔT was derived from GOES surface temperatures from 2 day-night periods (January 12-13 and January 18-19, 1981) for 1 area each in central and south Florida (Fig. 18). Area 4 (Fig. 17) is an agricultural area of drained organic soils, known as the Everglades Agricultural Area. Area 9 (Fig. 17) is in an area of excessively well-drained and well-drained sandy soils directly south of Ocala, in west north central Florida. Temperatures obtained from GOES images showed consistently that the well-drained and excessively well-drained areas are colder during winter nocturnal conditions and hence have different climate characteristics from wetland areas. Values obtained for inputs to the above equation and used to calculate ATI are listed in Table 17.

The difference in apparent thermal inertia (36.1 vs. 28.5) in value for organic soil from the same area and within a week may indicate that other factors (wind, atmospheric absorption) were neglected which could influence surface temperatures. Rainfall was scanty during the week of January 12-19, 1981. It ranged from 0 to a maximum of 0.18 inch, as reported in the Clewiston and Belle Glade area (Climatological Data, Florida, 85, January 1981). Diurnal surface temperatures for the Everglades Agricultural Area (Area 4, Fig. 17) for the 2 days showed a difference of 6°C during daytime (Fig. 18). This difference in surface temperature (increase in ΔT for January 18-19 compared to January 12-13) for the same area over a 6-day period caused the difference in the calculated ATI's. Wind data were insufficient to determine whether wind was a significant contributing factor to the temperature difference. We did not obtain vertical moisture profiles to correct for atmospheric absorption. One factor which may also contribute to the difference (6°C) in daytime surface temperature may be the extensive damage to crops in the area from the earlier freeze (January 12-13, 1981). This freeze killed leaves of the widespread sugarcane crop of the Everglades Agricultural Area, which would allow more solar radiation to reach the surface of the dark organic soil as well as reduce evapotranspiration from the vegetated surface. Thus, we conclude that moisture availability for evapotranspiration from the surface may affect thermal properties and perceived thermal inertia of the surface.

4.4.7. Spatial resolution and thermal properties

North of Lake Apopka in central Florida is a large area of organic soils. The temperature of this organic soil could not be resolved from the water temperature of Lake Apopka by the low spatial resolution of GOES. However, HCMM data symbol maps showed that these types of surface features were clearly discernible at the 0.6-km resolution. HCMM images (Fig. 19) showed that the water temperature of Lake Apopka was 10-11°C. A large area with a temperature of 2-3°C surrounds the lake; this area includes the cropped, drained, organic soil area and excessively drained

ORIGINAL PAGE 15
OF POOR QUALITY

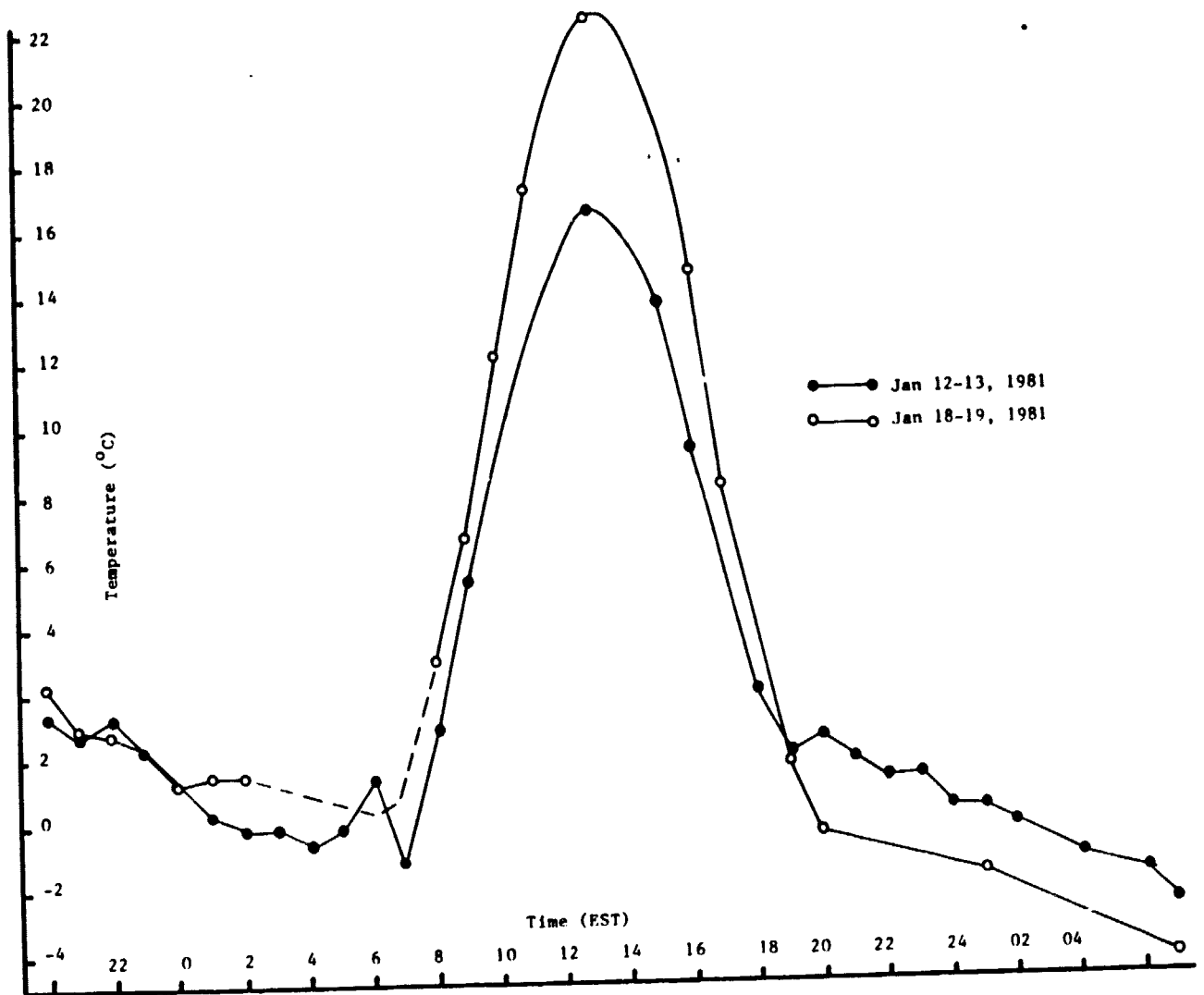


Fig. 18. Diurnal surface temperature (GOES) for the Everglades Agricultural Area (Area 4 in Fig. 17) for two days in January, 1981.

Table 17. Values used in calculation of apparent thermal inertia (ATI) for 2 areas in Florida: Area 4, the drained organic soils of the Everglades Agricultural Area (EAA) in South Florida, and Area 9, the area classified as excessively drained and well-drained mineral soils 25 km directly south of Ocala in the west North Central Florida peninsula. Data used were from January, 1981.

Area where ATI is calculated	Area 4		Area 9	
	Organic Soil		Mineral Soil	
Date (January, 1981)	12-13	18-19	12-13	17-18
N	1000	1000	1000	1000
θ (latitude)	26.5°	26.5°	29.0°	29.0°
ϕ (solar declination)	-21.63°	-20.58°	-21.63°	-20.58°
δ (hour angle)	-6°	-6°	-6°	-6°
C (Table 11-3, HCMM User's Guide)	0.981	1.004	0.926	0.950
ΔT (GOES), °C	19.3	25.0	24.6	23.1
r (reflection, from Geiger)	0.2	0.2	0.35	0.35
K (calculated from Eq. [3])	0.967	0.968	0.967	0.968
a (calculated from Eq. [2])	0.2014	0.2016	0.5370	0.5375
ATI (calculated) ^{1/}	36.07	28.51	17.42	17.56

^{1/} Unit for ATI is scaled to 0-255 rather than to physical units (HCMM User's Guide, p. 10).

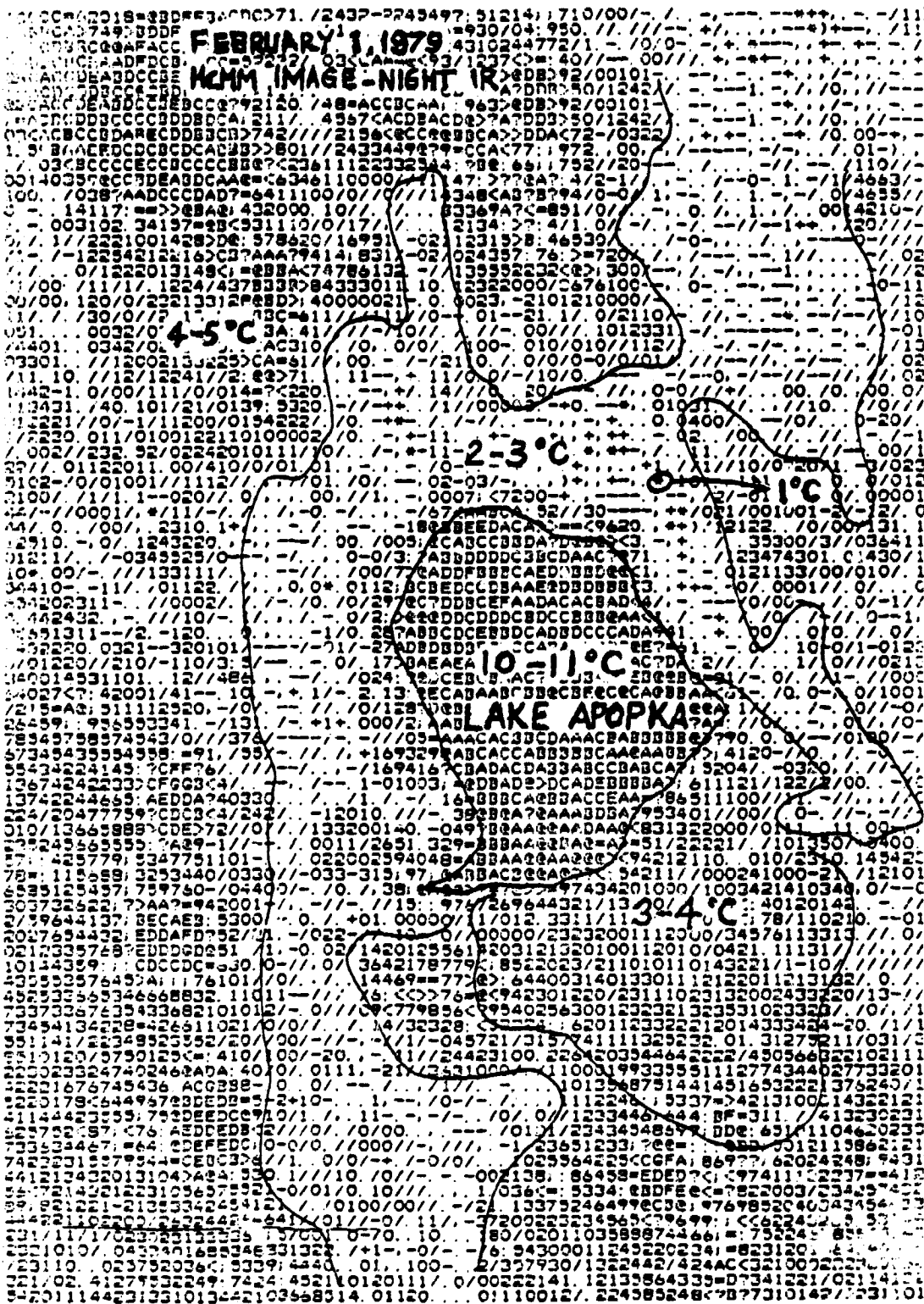


Fig. 9. HCCM night IR temperatures from Feb. 1, 1979, showing detailed (600 m resolution) land-water temperature boundaries in the Lake Apopka area.

sandy soil. Southeast of the lake is a large area with warmer temperatures (3-4°C). Farther north, near Gainesville, HCMM images showed that water temperatures of Newnan's Lake, Orange Lake, and Lake Lochloosa ranged from 8-10°C (Fig. 20), whereas the surrounding land surface temperature was 0-3°C. Payne's Prairie, a wetland area (marsh) southwest of Newnan's Lake, was 4-5°C. In both cases, the difference between land and water temperature was approximately 7°C. The GOES image (Fig. 21) showed 7°C (warmest) pixel for Lake Apopka and 3.5°C for surrounding areas. Newnan's Lake was not discernible at all in the coarse-resolution GOES imagery. The comparison of HCMM pixel resolution (0.6 x 0.6 km) with GOES pixel resolution (6 x 8 km) points out that there may be many small cold pockets or warm lakes within the coarse regional delineation that the GOES imagery gives for peninsular Florida.

4.4.8. HCMM thermal pattern of organic soil attributable to land use

A HCMM nighttime IR image (Fig. 22) of January 15, 1979, showed thermal patterns of lower Florida including the original Everglades marsh. The thermal image showed that although the soil base is the same, the different water contents on or near the surface resulting from different land use or management created the thermal patterns shown in Fig. 22. This pattern is also discernible in Fig. 2. The different surface water and near-surface water contents were partly due to different land use in the area, for example, agricultural (3), detention for water conservation (1 and 2), and natural (4) (Fig. 4). The Everglades Agricultural Area (3) generally contains the coldest areas in south Florida at night during winter cold weather conditions. The pattern of the agricultural area (Fig. 4) appears quite distinct in HCMM images (Figs. 5, 22).

It is obvious in comparing Fig. 22 (HCMM nighttime IR image) with Fig. 5 (HCMM apparent thermal inertia image) that drainage for agriculture resulted in colder nighttime surface temperatures mediated through a decrease in surface thermal inertia. Likewise, it is obvious that detention for water conservation results in an uneven surface water coverage as shown by sharp boundaries in the apparent thermal inertia in the organic soil area of the Florida Everglades.

4.4.9. Nocturnal surface temperatures, thermal inertia, and soil or surface properties

The climatic feature which usually separates the thin line between severe crop damage and little or no crop damage during winter cold air mass events in peninsular Florida is the temperature at the surface-atmosphere interface at night, and the length of time that it persists. Patterns of nocturnal low temperatures for 1979-80 and 1980-81 are shown in Fig. 23. These patterns bear a resemblance to both the apparent thermal inertia image (Fig. 5) and to the 5 thermal inertia classes superimposed on the General Soil Map of Florida (Fig. 12). First, in the northern half of the peninsula, the low nocturnal winter temperatures are largely associated with low thermal inertia patterns, which in turn are associated with the deep, sandy, well-drained soils of the Central Florida Ridge Land Resource Area (thermal inertia classes 1 and 2 of Fig. 12). Exceptions are generally related to areas with high densities of

ORIGINAL PAGE IS
OF POOR QUALITY

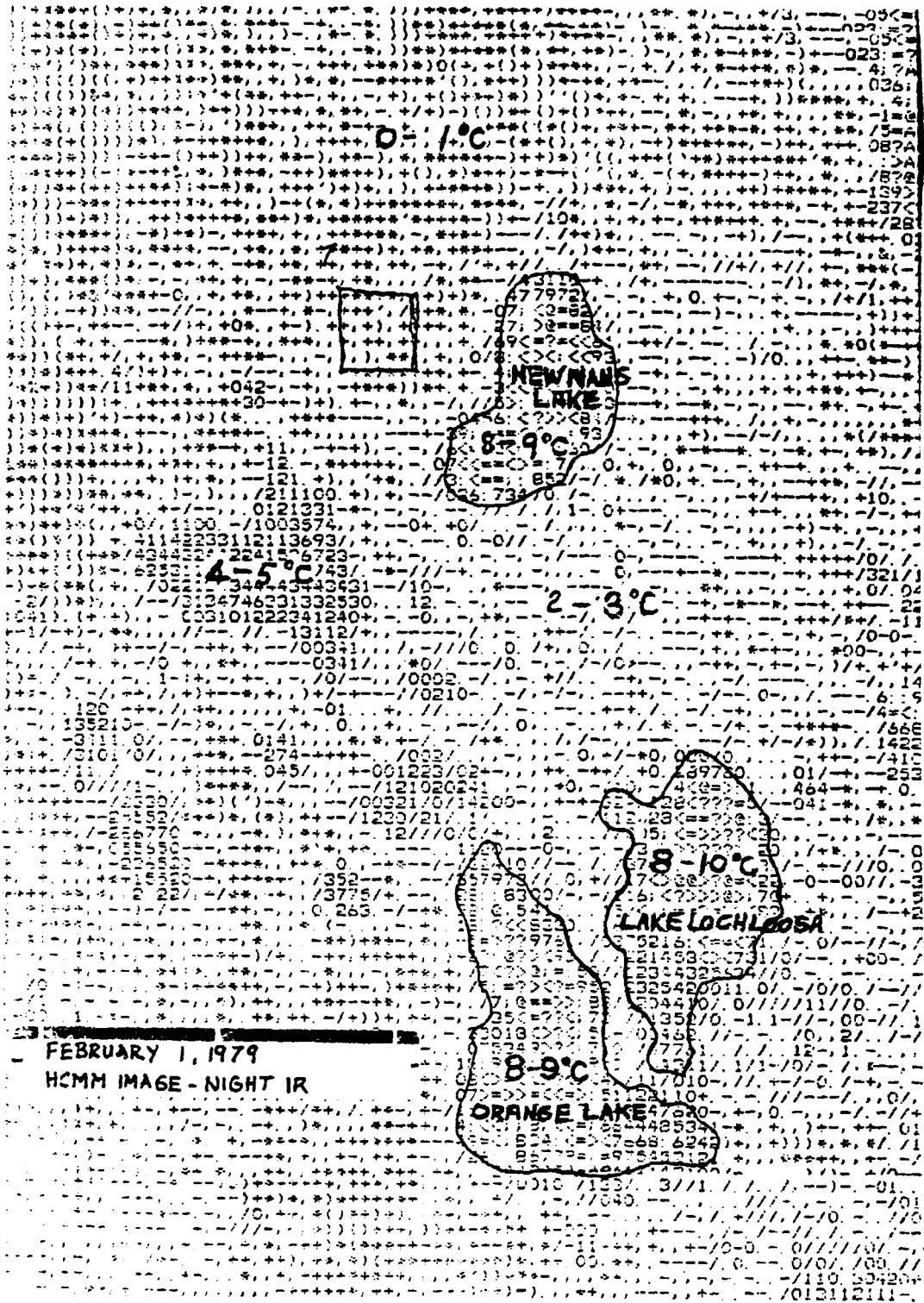


Fig. 20. HCMH night IR image of Feb. 1, 1979, showing detailed (600 m resolution) land-water temperature boundaries of Newnan's Lake area in North Central Florida.

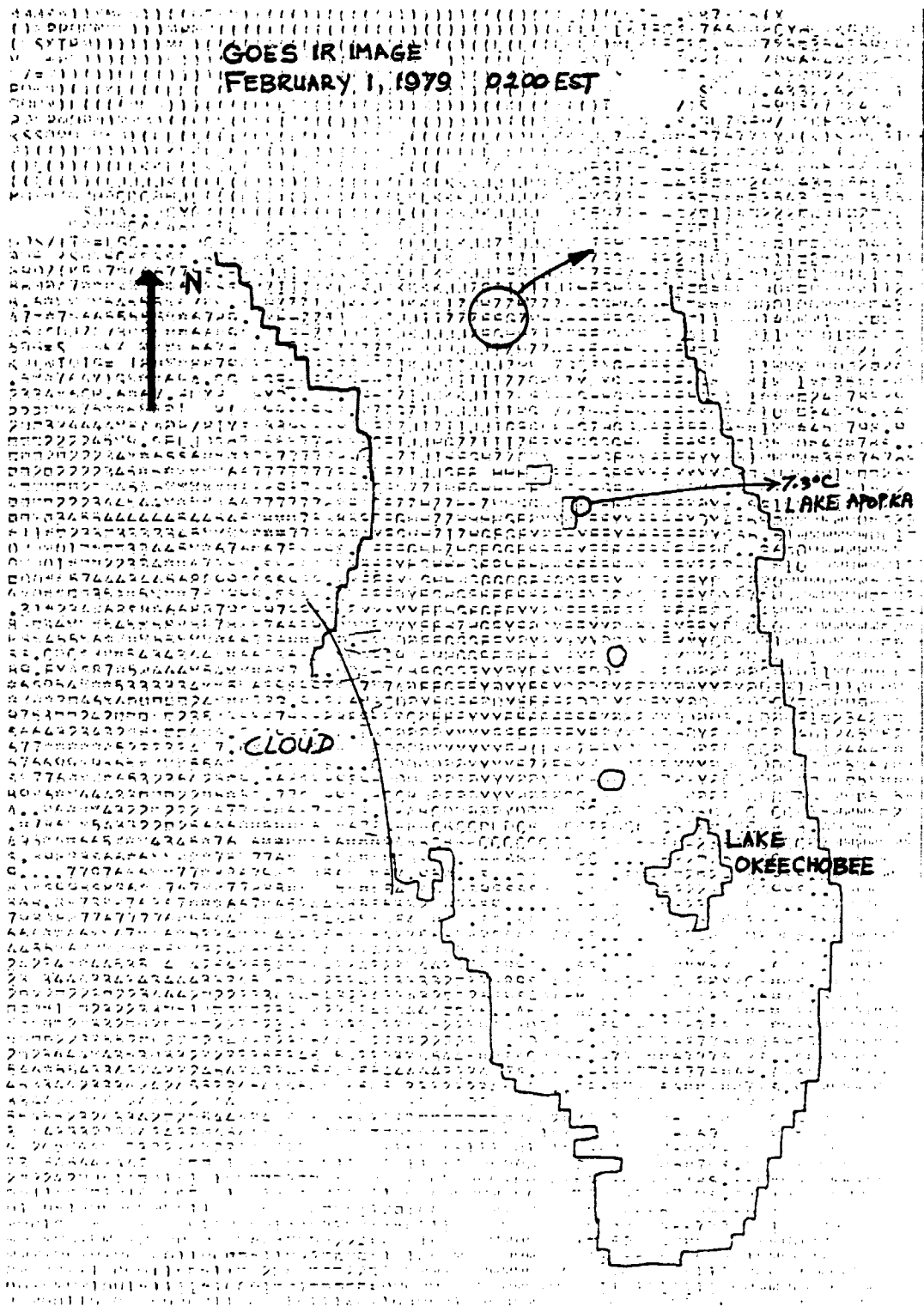
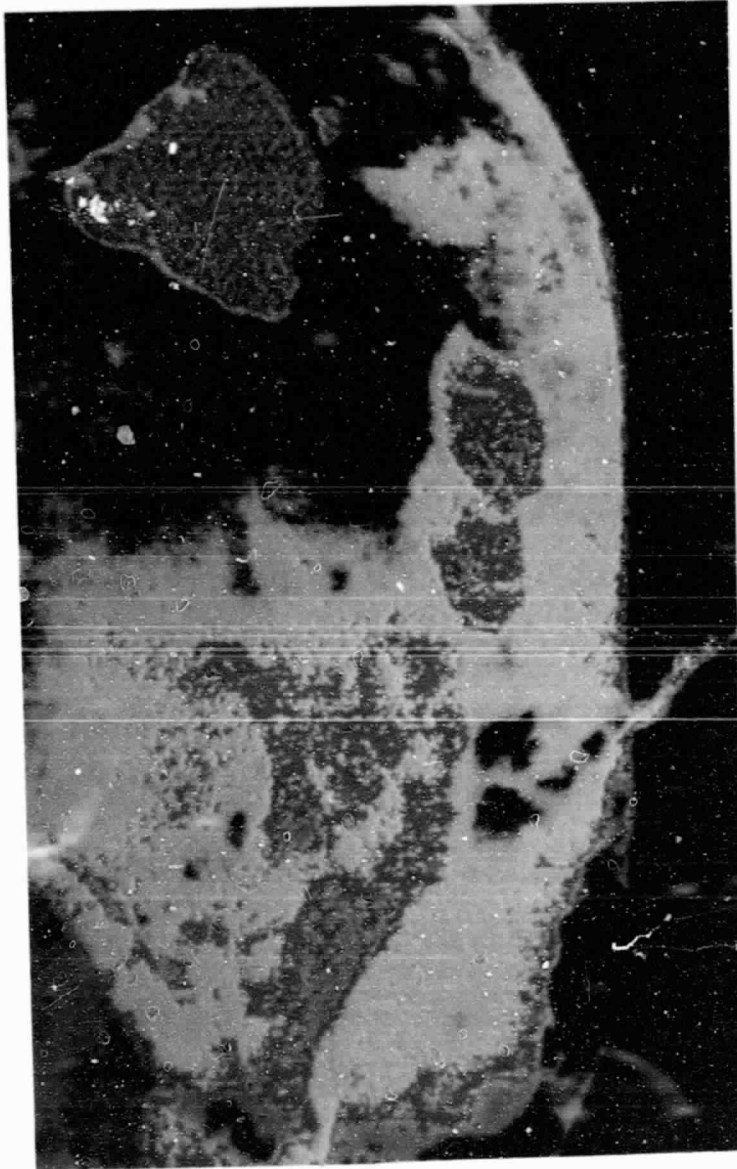


Fig. 21. GOES IR image of Florida from Feb. 1, 1979, 0200 EST, showing the land-water temperature boundaries for small lakes of 1 to 2 pixel area.

ORIGINAL PAGE IS
OF POOR QUALITY



Key

- | | |
|--------------------|--------------------|
| 1. Green (coldest) | 5. Magenta |
| 2. Orange | 6. Light blue |
| 3. Dark blue | 7. Black |
| 4. Yellow | 8. White (warmest) |

Fig. 22. HCMM nighttime IR image on Jan. 15, 1979, obtained by digitizing HCMM film transparence using the Image 100 computer at Kennedy Space Center. The image illustrates thermal patterns which can be generated due to different land use.

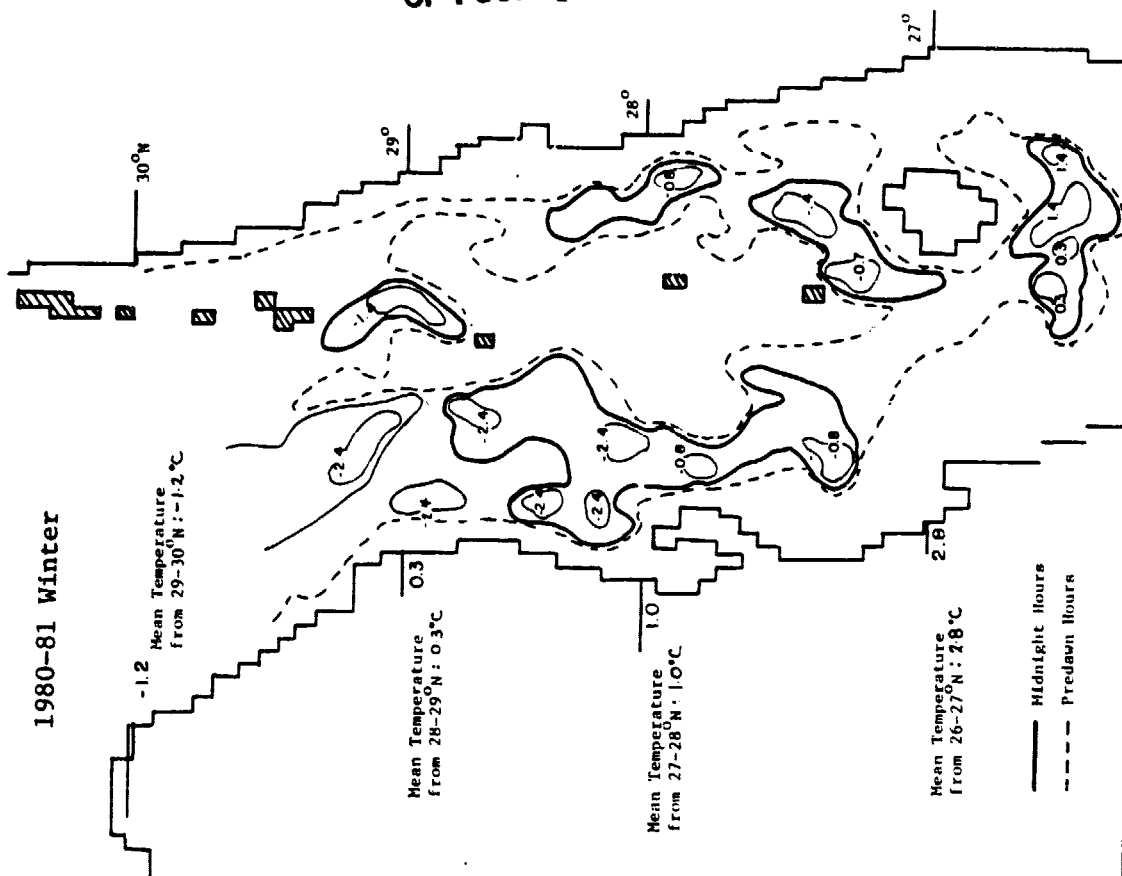
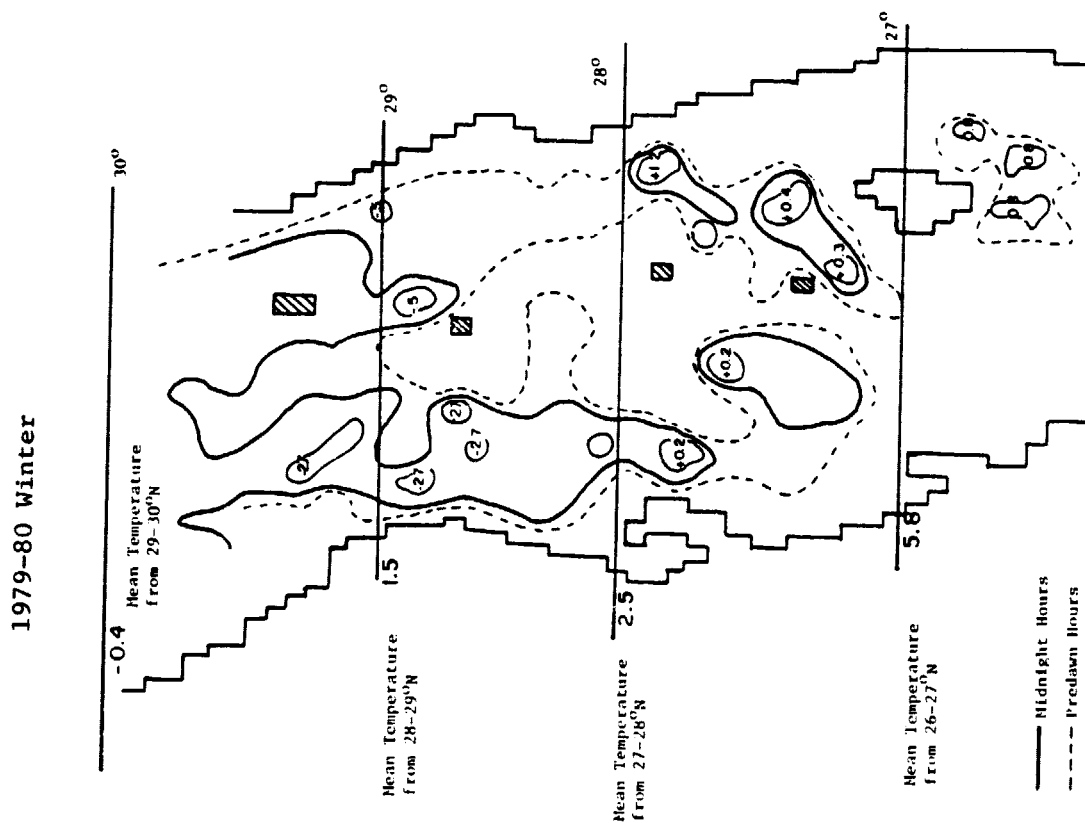


Fig. 23. Average low temperatures in the state during 1979-80 and 1980-81 winter seasons. Temperatures are in °C. Lines are time-expansion of cold areas initiated from cold areas. Thick lines indicate average coldest conditions during midnight hours and dashed lines indicate average coldest conditions during predawn hours.

lakes, which produce patterns of high thermal inertia although surrounding soils may have low thermal inertia. Second, a cold air area is usually found extending southward from the Tampa Bay Area in the western half of the peninsula. This area, although it is a part of the South Florida Flatwoods Land Resource Area, does have good natural (as well as manmade) surface drainage. Since 1978-79 was a wet winter, Fig. 5 shows only intermediate apparent thermal inertia. In the drier 1979-80 and 1980-81 winters, cold areas were present and persistent in the southwest peninsula.

Cold areas showed up north of Lake Okeechobee in 1979-80 and 1980-81 GOES data (Fig. 23) that had not been observed in three previous winters. These areas have naturally high water tables, but with dry weather coupled with artificial drainage for pastures, these small areas apparently decreased in thermal inertia and became relatively cold-prone.

South of Lake Okeechobee, the drained organic soil of the Everglades Agricultural Area appears as an isolated cold-prone area year after year. Sharp thermal inertia demarcations appear between the drained organic soil and the Water Conservation Areas.

In summary, we found broad agreement among patterns of HCMM apparent thermal inertia, cold-prone areas, and the soil drainage classes of the General Soil Map of Florida. Land use and management, especially drainage (or flooding) can alter thermal inertia and cold-prone relationships. Also, antecedent rainfall conditions can affect thermal inertia properties and cold susceptibility, especially of the South Florida Flatwoods Land Resource Area.

5.0. SUMMARY AND CONCLUSIONS

Generally cloudy sky conditions during the project period (1979) when HCMM data were available for thermal inertia studies in Florida caused us to depend more extensively on GOES temperatures than originally planned. The comparison of GOES data with the HCMM data had advantages because we found that the use of high resolution (HCMM, 600 m) versus low resolution (GOES, 8 km) data, and low frequency (HCMM, 36 hours) versus high frequency (GOES, hourly) data, permitted us to infer information not possible if we were restricted to either set of data alone. We were able to extend thermal inertia information for small areas (HCMM) to the peninsula (GOES), and were able to confirm GOES diurnal temperatures with HCMM data. Results from this project indicate that future work of this type should rely on both GOES and the high resolution polar-orbiting satellites (NOAA-6,7).

Future work should include improving the first order thermal inertia map generated in this project and refining land-water boundary effects of small lakes and coastal areas. The diurnal temperatures from GOES can then be investigated to yield more accurate thermal inertias for the state for use in specific small-area temperature predictive models for short-term forecasting of cold events.

Further summarization of results, accomplishments, significance, and recommendations is given in the Executive Summary.

6.0. REFERENCES

1. Carlson, T.N. and Boland, F.E. 1978. Analysis of urban-rural canopy using a surface heat flux/temperature model. *J. Appl. Meteorol.*, 17:998-1013.
2. Carlson, T.N., J.K. Dodd, S. Benjamin, and J.M. Cooper. 1981. Satellite estimation of the surface energy balance moisture availability and thermal inertia. *J. Appl. Meteorol.* 20:67-81.
3. Chen, E. 1979. Estimating nocturnal surface temperature in Florida using thermal data from geostationary satellite data. Ph.D. dissertation, University of Florida. 280 pp.
4. Chen, E., L.H. Allen, Jr., J.F. Bartholic, R.G. Bill, Jr., and R.A. Sutherland. 1979. Satellite-sensed winter nocturnal temperature patterns of the Everglades Agricultural Area. *J. Appl. Meteorol.* 18:992-1002.
5. Chen, E. and J.D. Martsof. 1981. The development of nocturnal GOES infrared data as a source of climate information. Final Report, National Climate Program Office, NOAA Contract No. NA80AA-D-00129. University of Florida, Institute of Food and Agricultural Sciences. 106 pp.
6. Chen, E., L.H. Allen, Jr., J.F. Bartholic, and J.F. Gerber. 1982. Delineation of cold-prone areas using nighttime SMS/GOES thermal data: Effects of soils and water. *J. Appl. Meteorol.* 21:1528-1537.
7. Chen, E., L.H. Allen, Jr., J.F. Bartholic, and J.F. Gerber. 1983. Comparison of winter nocturnal geostationary satellite infrared surface temperature with shelter-height temperature in Florida. *Remote Sens. Environ.* 13:313-327.
8. Chen, E., L.H. Allen, Jr. and J.D. Martsof. 1982. The application of geostationary satellite surface infrared irradiance temperatures to provide mesoscale climate temperatures. Final Report, NOAA Post-Doctoral Grant Contract No. NA81AA-D-00098. University of Florida, Institute of Food and Agricultural Sciences.
9. DuCharme, E.P. 1971. Soil temperature in Florida citrus groves. Tech. Bul. 747, Agric. Exp. Stat., Inst. Food & Agric. Sci., Univ. Fla. 15 pp.
10. Hanks, R.J. and F.L. Ashcroft. 1980. Applied Science Physics. Springer-Verlag, New York, NY. Advanced Series in Agricultural Science, No. 8.
11. HCMM User's Guide, 1980. NASA, Goddard Space Flight Center, Greenbelt, MD. Second Revision, October 1980. 120 pp.
12. Kimball, B.A. and Jackson, R.D. 1979. Soil Heat Flux in: Modification of the Aerial Environment of Plants. B.J. Barfield and J.F. Gerber, eds. ASAE, St. Joseph, MI.

13. National Oceanic and Atmospheric Administration, National Climatic Center. Climatological Data, Florida, Annual Summary, 82 (12) 1978, 83 (13) 1979, 84 (14) 1980, and 85 (15) 1981. Asheville, NC.
14. Price, J.C. 1980. The potential of remotely sensed thermal infrared data to infer surface soil moisture and evaporation. *Water Resources Res.*, Vol. 16, No. 4. pp. 787-795.
15. Rosema, A., J.H. Bijleveld, P. Reiniger, G. Tassone, K. Blyth, and G.J. Gurney. "Tell-Us," A combined surface temperature, soil moisture and evaporation mapping approach. 12th Int. Symp. on Remote Sensing of Environment. Manila, Philippines, April 20-26, 1978.
16. Soer, G.J.R. 1977. The Tergra model, a mathematical model for the simulation of the daily behavior of crop surface temperature and actual evapotranspiration. Niwars Publ. 46, Delft, Netherlands.
17. Soer, G.J.R. 1980. Estimation of regional evapotranspiration and soil moisture conditions using remotely sensed crop surface temperatures. *Remote Sens. Env.* 9:27-45.
18. Sutherland, R.A. 1980. A short-range objective nocturnal temperature forecasting model. *J. Appl. Meteorol.* 19:247-255.
19. Weinreb, M.P. and M.L. Hill. 1980. Calculation of atmospheric radiances and brightness temperatures in infrared window channels of satellite radiometers. NOAA Tech. Rep. NESS 80. 40 pp.